DRAFT!!! 8-15-99

# Communicating Across the Solar System

*C. D. Edwards and C. T. Stelzried, Jet Propulsion Laboratory,*
*California Institute of Technology, Pasadena, CA*

*(A Proposed Article for AES Magazine Issue for 50th Anniversary of IEEE-AES)*

## Abstract

One of the defining accomplishments of the 20th century is the beginning of our civilization's exploration of the solar system. The ability to communicate over solar system distances is one of the keys to enabling planetary exploration, and our deep space communications capability defines the bandwidth over which we can experience these remote worlds. The latter half of the 20th century reveals a remarkable growth in deep space communications based on sustained technology development and infusion of both flight and ground technologies. Future technology initiatives in the areas of higher frequencies, larger apertures, and improved coding promise further growth in deep space communications capability. Intensive *in situ* exploration of planetary targets such as Mars calls for the creation of new telecommunications infrastructures to create Internet-like functionality for support to future missions. These developments will transform the way in which we explore and experience the solar system in the coming millennium.

## 1. Introduction

In the last half of the 20th century, our civilization has begun the next chapter in our ongoing quest for discovery, with the initiation of the robotic exploration of our solar system. In less than fifty years, we have broken free of the Earth's gravity well and flown spacecraft to every planet in the solar system except Pluto. The ultimate goal of this exploration is to establish a virtual (and perhaps someday an actual) human presence throughout the solar system [NASA, 1988]. Clearly, communications is one of the central elements of creating such a virtual presence, and also one of the biggest technical challenges in planetary exploration. In this article we describe some of the key technology advances over this time frame that have enabled our planetary exploration to date, and we forecast how future communications technology breakthroughs will open the door to new levels of space exploration.

Deep space communication is fundamentally characterized by the enormous distances involved. A very simplified version of the communications link equation highlights this challenge:

$$R \propto \frac{P_t A_t A_r}{\lambda^2 L^2 T_{sys} SNR_{req}^{bit}}$$

where

| | |
|---|---|
| $R$ | is the achievable data rate, |
| $P_t$ | is the transmitted power, |
| $A_t$ | is the effective area of the transmitting antenna, |
| $A_r$ | is the effective area of the receiving antenna, |
| $\lambda$ | is the wavelength of the radiated signal, |
| $L$ | is the distance between transmitter and receiver, |

$T_{sys}$ is the system noise temperature of the receiving system, and

$SNR_{req}^{bit}$ is the required bit signal-to-noise ratio.

The factor of $L^2$ in the denominator implies that the achievable data rate of a given telecommunications system scales inversely with the square of the communications distance.

To put this in perspective, note that when the Voyager spacecraft encountered the planet Neptune, it was roughly 30 Astronomical Units from Earth, or about 4.5 billion kilometers. Contrast this link with a typical geostationary communications satellite, 40,000 km above the Earth's surface. The distance for these two scenarios varies by more than a factor of 100,000, implying that the communications challenge for the link from Neptune is *ten orders of magnitude* larger than for the geostationary link.

This same link equation also provides the key to the technologies that make it possible to achieve significant data rates on deep space links, in spite of this enormous distance penalty. Reading through the various factors in the equation, it is clear that deep space communications is enabled by a combination of advancements in:

- High power spacecraft transmitters
- large effective aperture spacecraft antennas
- large effective aperture ground antennas
- moving to higher frequencies
- reducing system noise temperature
- optimizing channel coding and modulation schemes to minimize the signal-to-noise ratio required to achieve a given bit error rate.

We will see throughout this paper how progress in each of these areas has helped to create the deep space communications capability we have today, and how further breakthroughs in each of these areas point the way towards tomorrow's capabilities.

In addition to the clear impact of large distances on communications performance, three other aspects of deep space missions provide unique challenges for the design of telecommunications systems, relative to terrestrial and near-Earth systems. First, an additional consequence of the large distances of interplanetary links and the constant speed of light is long signal propagation times. The round trip light time varies from roughly 10-40 min between Earth and Mars, reaches nearly two hours between Earth and Jupiter, and exceeds 8 hrs between Earth and Neptune. These long round-trip light times make it impossible to "joystick" interplanetary spacecraft from Earth, driving the need for high levels of onboard autonomy, and also prevent the use of the kinds of two-way protocols typically used in terrestrial applications to deal with communications channel variability.

A second feature of deep space missions is the wide range of environmental conditions experienced across the mission set. With mission targets ranging from close to the sun out to Pluto and beyond, spacecraft communications systems encounter vastly different thermal environments. Spacecraft near Jupiter can encounter multi-Megarad radiation levels. And penetrators like the New Millennium DS2 Microprobe mission to Mars experience enormous acceleration and shock levels. These unique environmental challenges place rigorous demands on flight system components.

A final distinguishing aspect of deep space missions is the extreme emphasis on low-mass systems, driven by the high cost-per-unit–mass of delivering payloads to interplanetary targets. Thus, while the link equation suggests the need for high power, large aperture spacecraft communications systems, the economics of payload launch costs pushes back in the direction of highly efficient, low-mass systems. Additional constraints on flight systems are imposed by launch vehicle constraints on payload volume. The telecommunications system designer must carefully balance these competing factors of cost, performance, mass, and volume.

In the remainder of this article, we will summarize the early history of NASA's Deep Space Network (DSN), highlight some of the key technological developments over the DSN's evolution, describe the capabilities of today's DSN, and examine some of the key future directions for the development of new enhancing and enabling deep space communications capabilities for the new millennium.

## 2. Early History of the Deep Space Network

### *2.1 A World-Wide Deep Space Network from a Small Beginning*

The NASA/JPL Deep Space Network (DSN) is a continuously evolving worldwide deep-space telecommunications network (Renzetti 1971). The pre-DSN effort drew from JPL post-World War II U.S. military sponsored communications and radio astronomy research (Corliss 1976). A large scale deep space network must continually support multiple spacecraft at distances to the edge of the solar system with both high power command uplinking and downlinking telemetry for engineering, science and radio metric data. This capability typically requires numerous large antennas with multiple low-noise pre-amplifier receiving systems, highly stable and accurate frequency and timing systems, and high power uplink transmitters all operating at microwave frequencies. They are deployed world-wide, with appropriate data storage and transfer systems as well as scheduling systems supporting prioritized users (Reid, et al 1973, Posner and Stevens 1984). The present DSN, with NASA support, has achieved many orders of magnitude performance improvement since the first pre-DSN 26 m diameter polar mount antenna was completed in 1958 at the Goldstone, CA Pioneer station (Rafferty, et al 1994).

Rocket propulsion experiments in the 1930's led to the formation of JPL, a division of the Pasadena, California Institute of Technology (CIT) in 1944. Dr. Theodore von Karman was the original JPL president (Koppes, 1982). These early experiments led to the development of jet-assisted take off for airplanes (JATO) and in 1949, the Corporal missile was selected for development as the first U.S. guided missile weapon system. Important technologies, including in-flight telemetry instrumentation, antenna, and rf components developed for the Corporal missile were most useful for future space flight and planetary exploration. In January 1958, JPL's Microlock ground system (Fig. 2-1), consisting of helix antennas developed for the Army, successfully tracked the first U.S. earth satellite Explorer 1. This satellite ground system operating at 108 MHz was credited with discovering the Earth's Van Allen radiation belts (Corliss, 1976). The phase-lock loop concept (Jaffe and Rechtin 1955) used in this early JPL receiver for reception of the weak signals typical of deep space missions has been used by all the missions to date for deep space communications (Yuen, 1983 pp. 50).

Figure 2-1. The Deep Space Network precursor, JPL's Microlock system composed of 5-foot-long helical antennas, tracked Explorer 1.

NASA was established in October 1958, and consolidated the United States military space program into a civilian organization. JPL was transferred to NASA from the Army in December 1958 and made responsible for the lunar and planetary exploration programs. In 1958, the Goldstone (Linnes, et al 1960, Stevens 1961) 'receiving station' (subsequently renamed the Pioneer station and designated DSS 11) became the first DSN 85 foot (26-m) diameter large ground antenna. It was built in seven months by the Blaw-Knox company using an existing radio telescope design with a polar mount (Fig. 2-2).

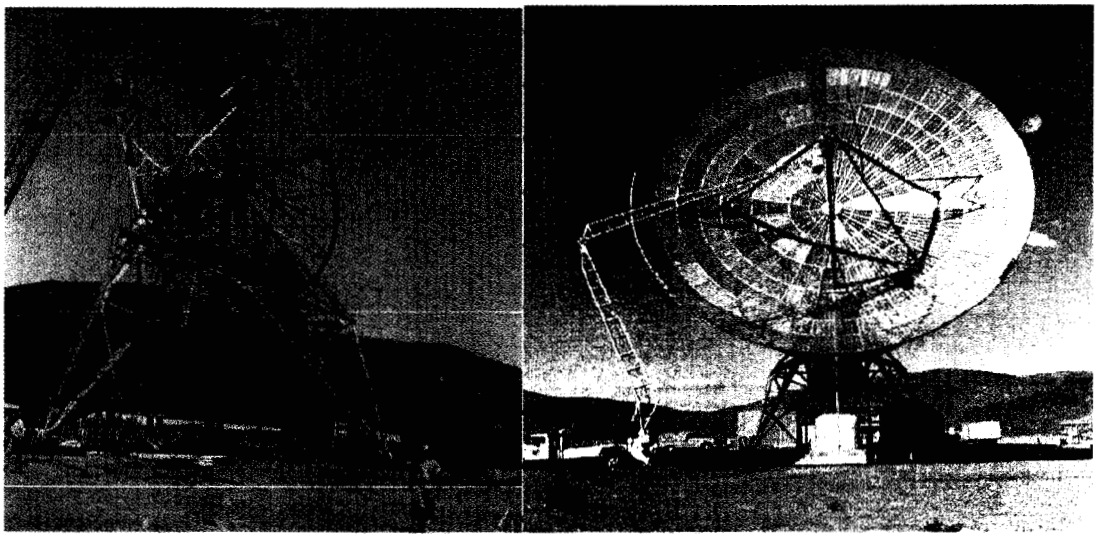

Fig. 2-2. Photographs of the under-construction and completed Goldstone 'receiving station' (later called the Pioneer station or DSS 11), 85 foot (26-m) diameter polar mount antenna, completed in November 1958.

## *2.2 The Beginning of the DSN*

The purpose (Rechtin, 1959) of this antenna was to track the Pioneer 3 (launched December 1958) and Pioneer 4 (launched March 1959) spacecraft at 960 MHz. Pioneer 3 achieved near Earth orbit and discovered the second Van Allen radiation belt before failure. Pioneer 4 escaped the earth to achieve solar orbit. The receiving station antenna, the Puerto Rico station small antenna, the Cape Canaveral launch center, and the Cape Canaveral and JPL message centers formed an early Tracking Network (Corliss, 1976, Figure 3-1). This early system was important as a foundation for the growth of the DSN (Waff, 1993). The Pioneer station was decommissioned in 1981 and designated a national monument in 1985.

In February 1960, the Goldstone 'transmitting' station (subsequently renamed the Echo station and DSS 12) was completed using an azimuth-elevation (az-el) mount. It became the second future DSN 85 foot (26-m) diameter large antenna Its purpose was to use two large 26-m diameter antennas to support the joint Bell Telephone Laboratory and JPL Project Echo experiment (Stevens and Victor, 1960). These experiments used a 100 foot diameter passive satellite reflecting balloon in orbit at 1000 miles altitude. This was the largest man-made object placed in orbit around the earth at that time. Bell Telephone Laboratory also had transmitter and receiver antenna systems on the East coast. The Goldstone communications portion of the experiment operated with a 10 kW S-band (2390 MHz) transmitter for West to East and an L-band (960 MHz) receiver for East to West reception. Signals were cooperatively and successfully bounced off the reflecting Echo 1 balloon in both directions, between the East and West coasts using both sets of antennas, completing the experiment in August 1960.

The availability of the two new large antennas, the Echo station antenna for transmitting a 13-kW CW signal and the Pioneer antenna for receiving the signal provided the opportunity for the first planetary radar experiments. The sensitivity of the Pioneer antenna was improved with the addition of an S-band maser LNA as discussed in section 3.3. During 1961, this powerful radar system performed the first successful planetary radar (Victor and Stevens, 1962) with the detection of a Venus return signal. A key result was improving the accuracy of the Astronomical Unit which allowed improved deep space navigation and eventually improved the scientific value of the Mariner-2 flyby of Venus. These radar experiments have continued to the present with many exciting results from both planets and other solar system objects including asteroids. Some of the radar experiments have been coordinated with various missions, such as establishing landing sites for the Viking Landers and Pathfinder Mars missions.

### *2.3 Pre-DSN First Subnet for Tracking the First Missions*

During 1961-1962, with lunar probe spacecraft Rangers 1 through 5 and with the follow-on missions need for world wide tracking coverage, the 26 m diameter polar mount antennas were also built in Woomera, Australia and Johannesburg, South Africa. This completed the first 26 m antennas subnet. These 960 MHz antenna and receiver systems, designated collectively as the Deep Space Instrumentation Facility (DSIF) included a diplexed transmit/receive capability (Corliss, 1976, Tables 4-1 to 4-3). The deep space network (DSN) at that time consisted of the DSIF plus ground communications and data processing capabilities.

### *2.4 Technology Improvements through Science Support and the NASA Advanced Systems Program*

In 1962, a new 26-m diameter polar mount was built at the Goldstone Echo station as a replacement for the original 26-m az-el mount antenna. The Echo station 26-m az-el mount antenna was then moved to the Venus station in the summer of 1962 for research applications . The Venus Station, called DSS-13, served as a test facility that enabled thorough tests of new technology for extended periods. This extensive testing proved to be very valuable.

Equipment demonstrated at DSS-13 included microwave feed system components that operated at transmit power levels up to 500 kW CW while supporting ultra-low-noise receiving equipment. Also included were transmitters, cryogenically cooled low-noise amplifiers, receivers, frequency/time standards and distribution systems, and station automation systems. End-to-end system level tests in the field provided integration test results and system knowledge that could not be obtained in laboratory tests of equipment. These included evaluation and testing of future deep space communications systems as well as performing various science experiments including radio astronomy and planetary radar (Goldstein 1968).

As stated previously, the Pioneer station 26-m diameter antenna was first used to support the Pioneers 3 and 4 missions. This was performed with 960 MHz receivers and mixer front ends which had noise temperatures on the order of 1500 kelvins. The sensitivity of these early systems were considerably improved with the addition of receiver pre-amplifiers using parametric low noise amplifiers (LNAs) and later lower noise maser LNAs (Sato and Stelzried 1962). Although this technology was a good start toward the development of the improved sensitivity required of the future DSN for deep space tracking and science support, it was quickly realized that the DSN should be carefully planned, tested and created to reduce noise and interference. This would require a diverse workforce with a wide range of skills and interests. This challenge was aided by scientists and engineers excited with new possibilities for these future large antennas not only as needed for space communications but for parallel scientific purposes including planetary radar, radio astronomy and radio science.

Five years after the Pioneer station antenna was completed and a world wide network of 26 m diameter antennas completed, the DSN was officially established in December 1963 (Corliss 1976).

The ground system requirements were driven by the space exploration missions, but other scientific projects such as planetary radar were accommodated by the DSN with faster system development and verification than was possible by other means. Although this synergy of mission needs continues, it was recognized that an official deep space technology development effort should be formed. Therefore, in 1963, the NASA established the Advanced Systems Program for research and development of the future DSN. This program sponsored the research and development of all the important areas required for deep space telecommunications, including antennas, low noise amplifiers, receivers, coding, and frequency and timing.

For the purposes of this paper, the early DSN history in this section ends in 1963, when the DSN was officially established. This history, is continued in the following sections. DSN and deep space missions key events are listed in chronological order in Appendix A.

# 3. Key Technology Developments Over DSN's History

## *3.1 Large aperture ground antennas*

A second 26-m diameter antenna S-band DSN subnet was completed in 1965. This consisted of the Goldstone Echo station new 26-m diameter polar mount antenna completed in 1962 and new 26-m diameter polar mount antennas at Tidbinbilla, Australia and Robledo, Spain. These antennas provided additional S-band support and scheduling flexibility for the anticipated Surveyor, Lunar Orbiter and additional Mariner missions. The three complexes are spaced with nearly equal Earth longitude spacing, providing continuous overlapping coverage.

The improvements of the DSN spacecraft-link performance continued with the changeover from L to S-band to support the Mariners 3 and 4, the first S-band missions. This changeover was completed in 1965 while supporting L-band legacy missions. The DSN then supported the Mariner 4 Mars flyby in July 1965.

Construction and completion of the Goldstone Mars site 64-m az-el mount antenna initiated in 1963 is shown in Fig. 3.1. The first signal of the completed antenna (Fig. 3.1) was received from Mariner 4 in 1966. Both the Tidbinbilla (near Canberra), Australia (DSS 43) and Robledo (near Madrid), Spain (DSS 63) station's 64-m antennas were completed in 1973. Completion of this subnet of larger antennas with a single S-band feedcone greatly increased the sensitivity and performance of the DSN. Next, the 64-m antenna subnet was upgraded with 3 separate feedcones for greater flexibility. Each feedcone had separate feed and electronics (Stelzried, et al 1968). One of the feedcones was reserved for science applications. With the off-axis feeds now forming a circle, the system antenna gain is optimized by tilting and rotating the subreflector for feed selection. In 1973 the Goldstone 64-m antenna microwave optics were further upgraded with a dichroic frequency selective all aluminum plate over the X-band feed and an ellipsoidal reflector over the S-band feed, thereby allowing simultaneous reception of both S-and X-bands as well as S-band uplink (~2115 MHz). This dual-frequency capability was verified at Goldstone and added to the overseas antennas.

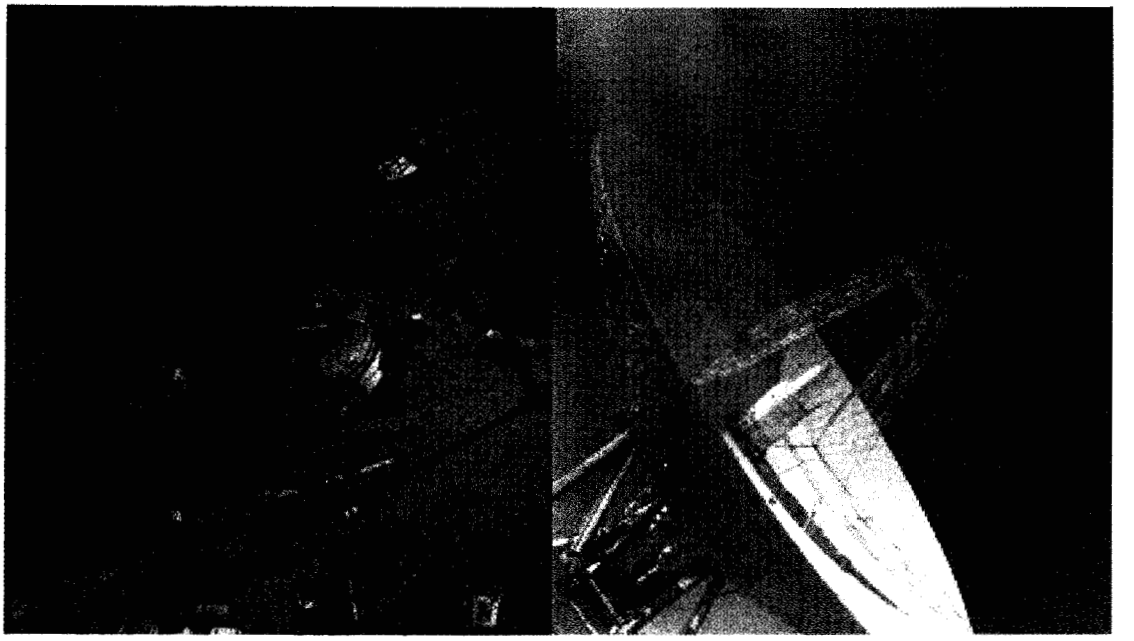

Fig.3-1. Photographs of the construction and completed Goldstone 210-foot (64-m) diameter az-el mount antenna prior to the first reception on March 1966 when Mariner 4 was approaching solar occultation (JPL photo #s 333-3820BC and 332_8645A)

Three DSN 26-m diameter polar mount antennas were expanded to 34-m diameter and X-band receive capability was added by 1979. These were designated 'standard' (STD) DSN antennas, providing simultaneous reception of S-and X-bands as well as 20 kW S-band uplink.

A subnet of 34-m shaped dual reflector DSN antennas called High Efficiency (HEF) antennas, with improved X-band performance relative to the earlier 34-m diameter antennas, was built for the three DSN complexes. This S-and X-band antenna subnet was completed prior to the January 1986 Voyager Uranus encounter. The S-and X-band simultaneous receive and simultaneous S-or X-band uplink 20 kW capabilities were achieved using a common aperture feedhorn.

The 64-m diameter subnet antennas were upgraded to high efficiency 70-m diameter dual shaped reflector antennas with overall improved sensitivity performance of 2 dB at X-band (Fig. 3-2) as well as retaining the flexible usage of the multiple feed cone capability. This large and very difficult world wide task was completed in 1988 with only 6 months downtime at each complex, and in time for the August 1989 Voyager Neptune encounter. Microwave holographic imaging was used to adjust the nearly 2000 individual reflecting panels on each of the three 70-m diameter antennas.

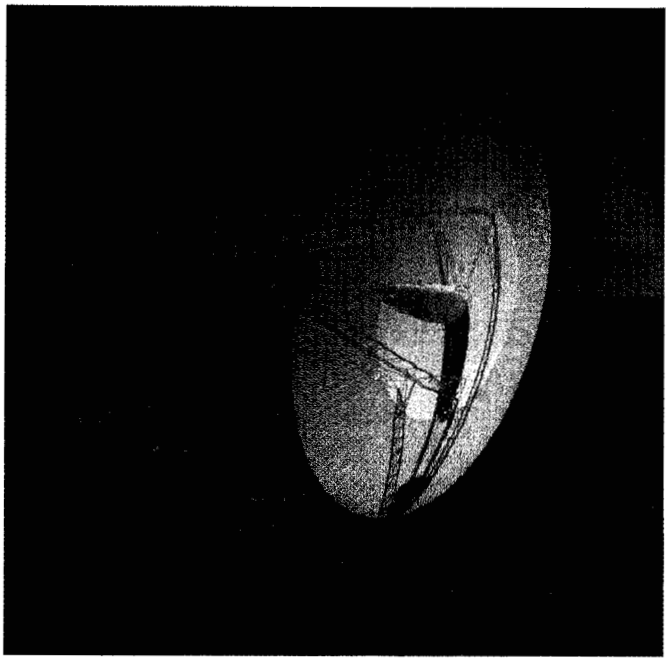

Fig. 3-2 Photograph of the Goldstone Mars station (DSS 14) antenna after the 1988 completion of the 64 to 70-m diameter antenna upgrade.

The 1989 Voyager 2 Neptune encounter was supported by arraying multiple DSN and non-DSN antennas resulting in nearly 8 dB link performance improvement relative to a single earlier 64-m diameter antenna (Layland and Brown 1985).

The Goldstone Venus station (DSS 13) research antenna was used to verify the benefits of a beam waveguide (BWG) antenna concept. This new research antenna was completed in 1991 (Fig. 3-3). These antennas use the large beam waveguide with multiple mirrors to route the microwave energy from the subreflector to a large pedestal room beneath the antenna, where the feeds and electronics are housed. The BWG configuration provides lower cost maintenance, more stable operating conditions and multiple separate low noise amplifiers, receivers and transmitters for greater reliability and versatility. This concept was transferred to the operational DSN and installed on the 34-m diameter BWG antennas at the three DSN complexes. The DSS 13 research BWG antenna is also being used to demonstrate the advantage of increasing future DSN frequencies to Ka-band (32 GHz); this is discussed further in the next section of this report.

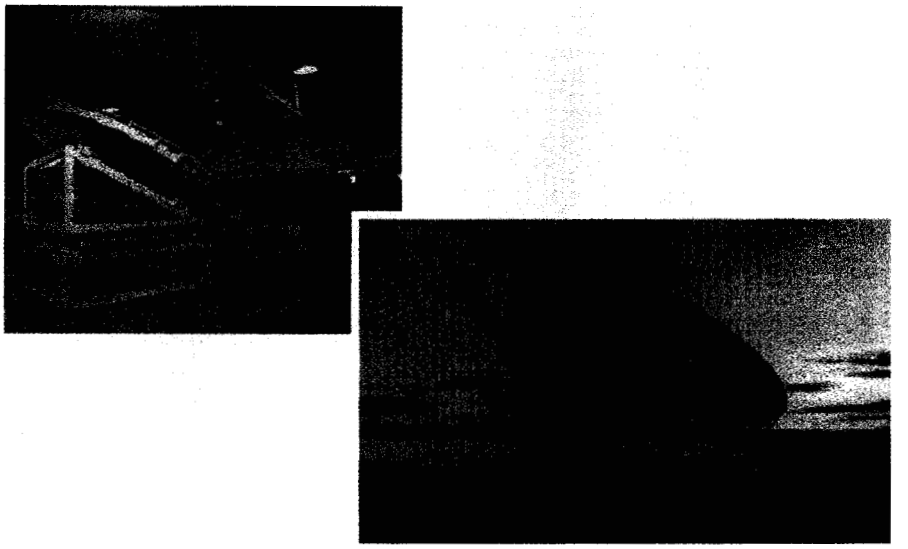

Fig. 3-3. Photograph of the Goldstone Venus station (DSS 13) research 34-m diameter az-el mount beam waveguide (BWG) antenna and the large pedestal room with reflecting mirrors and electronics (JPL photos; UL: 15839BC, LR: 15720BC).

With the availability of the newer 34-m BWG antennas, and with increasing maintenance costs, the older polar mount 'standard' antennas are being decommissioned, starting with the Goldstone DSS 12 antenna. In October 1996, this antenna was made available to the Apple Valley Science and Technology Center. The Goldstone-Apple Valley Radio Telescope (GAVRT) activity provides new usage of this resource for public school educational use.

The present DSN deep space antenna inventory, consisting of 12 operational antennas at both S-and X-bands, is discussed in section 4.

### *3.2 Extremely sensitive low-noise receivers*

From the communications link equation, the requirement to communicate with interplanetary spacecraft at great distances emphasized the need for large earth-based antennas with high power transmitters and sensitive low-noise receivers. The spacecraft portion of the telecommunications link experiences practical limits on antenna size and transmitter power. A resulting need for low system operating noise temperatures was recognized early in the pre-DSN era. Early receiving systems were dominated by high receiver noise with resulting reduced sensitivity.

Maser work was initiated in 1955, with initial emphasis on the development of an ammonia maser. Professor J. Weber had published an article in 1953 that indicated the inversion of the population of a quantum-mechanical energy-level system could be used for amplification. Professor N. Bloembergen of Harvard University published his proposal for a three-level maser using electron paramagnetic resonance in 1956. Walter Higa's JPL group demonstrated a 960 MHz cavity maser using ruby in the laboratory in 1959, following the Bell Laboratories success with solid-state masers and the first use of ruby as a maser material at the University of Michigan.

A 960 MHz cavity maser was installed at the prime focal point of a 26-m antenna at the 'receiver' site during September 1960 for a demonstration. A 2388 MHz cavity maser was installed at Pioneer site in February 1961 for the Venus Radar Experiment (Victor and Stevens 1962, p.84). These masers used liquid helium for "open-cycle" cooling.

Several cavity masers using open-cycle cooling were used on 26-m antennas at Goldstone tracking stations during the period between 1960 and 1965. Development of the DSN's traveling wave masers (TWMs) began in 1962 and continued for over twenty years, providing a variety of S-and X-band amplifiers. Reflected-wave masers operating between 19 and 25 GHz were developed during the 1970s for radio-astronomy applications.

Early developments important to the DSN's use of ruby masers included the Cryodyne (a closed-cycle refrigerator produced by A. D. Little, Inc.), an improved closed-cycle refrigerator developed at JPL (Higa and Wiebe, 1967), and comb-type slow-wave structures for traveling-wave developed by Bell Telephone Laboratories, Airborne Instruments Laboratories, and by JPL.

Technology developments to reduce the maser's effective input noise temperatures continued throughout the history of the DSN. Maser noise temperatures values of 2.1 K at 2295 MHz were achieved in 1974 for the reception of TV pictures at a 117 kb/s data rate from Mariner 10 near Mercury (Clauss and Wiebe 1975). X-band masers with noise temperatures of 3.5 K were developed to enhance Voyager encounters at Saturn in 1980 and 1981, Uranus in 1986, and Neptune in 1989 (Clauss and Quinn 1983). Fig. 3-4 shows the slow-wave structure and isolaters (left), the microwave input waveguide assemble (middle), and the assembled X-band maser (right).

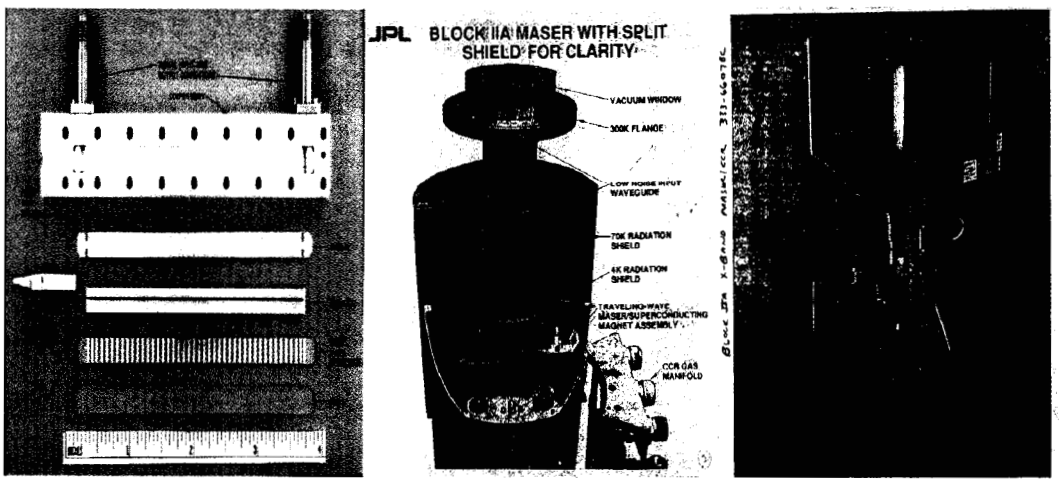


Fig, 3-4 Photographs of the JPL X-band TWM comb structure, microwave input, and packaged system ready for installation in the antenna feedcone.

A DSN S-band maser with a 2.5 K noise temperature was used in the Usuda 64-m antenna to support the International Cometary Explorer (ICE) mission in 1986 and the Voyager Neptune encounter in 1989. Usuda's beam waveguide (BWG) antenna G/T performance with the S-band maser was 2 dB better than the DSN's 64-m antenna at the time. This demonstrated that the use of beam waveguide need not degrade antenna performance compared to Cassegrain configurations. The BWG configuration provides protection for critical feed components during rain, enabling lower noise performance than a Cassegrain antenna during wet weather.

Cryo-cooled High Electron Mobility Transistor (HEMT) preamplifier assemblies have been built by JPL and purchased from private industry. Development work with cryo-cooled HEMTs indicates that maser-like noise temperatures will be approached in the future. Lower purchase and maintenance costs makes the HEMTs very attractive for use in the DSN. Recent photographs taken in 1998 in Fig. 3-5 show an X-band cryo-cooled HEMT module and the cryo-cooler vacuum housing being prepared for the DSS-34 Australian station's BWG antenna. At this time about half of the DSN's 44 cryo-cooled LNAs are HEMTs.

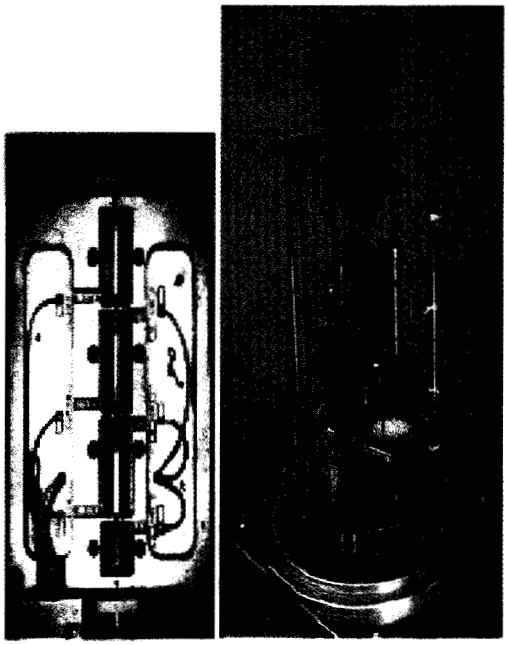

Fig. 3-5 Photographs of the JPL HEMT module and a single channel HEMT low noise cryogenic X-band microwave configuration with vacuum housing and radiation shield removed.

Masers, however, are still used to supply the lowest noise performance required for the most critical applications, particularly at the higher frequencies. Progress with masers at 33.7 GHz and 32 GHz continues. A 33.7 GHz dual cavity, dual polarization maser is currently in use at DSS-13 for spectral line radio astronomy. The 33.7 GHz maser has a cooled feed system. Earlier use of the 2-cavity maser for tracking Mars Observer Ka-band beacon at 33.7 GHz demonstrated a maser noise temperature of 5 K at the feed-horn aperture (Shell 1994).

### *3.3 Migration to higher frequencies*

The communications link advantage for migrating to a higher frequency occurs when area-limited antennas are used at both ends of the link. With a fixed spacecraft antenna size and a fixed ground antenna size, up to 11.3 dB improved link performance is theoretically available at X-band (8.42 GHz) compared to S-band (2.295 GHz). This is due to the higher energy density in the narrower downlink beam at the higher frequency. It was verified that the DSN would perform well at X-band (Petty and Clauss 1968). X-band was flown as an experiment on the deep space Mariner 10 (Howard 1974) and Vikings

(Michael, et al 1977) missions, and it's performance verified. It was used with the Voyagers for the prime communications link.

The addition of Ka-band (32 GHz) to the DSN continues the strategy to exploit the advantage of higher frequencies. The advantage of Ka-band (32 GHz) relative to X-band (8.42 GHz) of 11.6 dB is attractive. However, higher atmospheric losses at Ka-band reduces the advantage considerably, depending on the site location. An averaged DSN worldwide link advantage is about 6 dB (Edwards et al 1999). Some of this link performance degradation is also due to the current reduced antenna performance at this higher frequency in the DSN. This 6 dB 'data capacity' advantage for the ground systems assumes equal spacecraft effective antenna areas and transmitted downlink power with frequency. Accounting for the current spacecraft actual effective antenna sizes and transmitted downlink power performance at Ka-band relative to X-band reduces this advantage in the near term by several dB. Future missions will use Ka-band when the DSN ground antennas are implemented and spacecraft improvements are sufficient to justify the additional mission costs associated with this new communication frequency.

Table 3-1 lists the various frequencies used by the deep space mission spacecraft (S/C) and DSN for communications and scientific research (not including an expanding list of DSN radio astronomy frequencies from 1610 MHz to 115 GHz).

| Frequency Band* | Frequency, MHz | Propagation Direction | Application | Time Period |
|---|---|---|---|---|
| L | 960 | Downlink up/down | S/C communications or Radar | 1958-1965 |
| L | 890 | Uplink | S/C communications | 1958-1965 |
| L | ~1670 | Downlink | S/C communications (1) | 1985-1986 |
| | 1600-1720 | Down | or SVLBI (2) | 1997-2005 |
| S | 2388 | up/down | Radar (3) | 1961-1976 |
| | 2320 | up/down | Radar (3) | 1976- |
| S | 2290-2300 | Downlink | S/C communications (4a) | 1963- |
| S | 2110-2120 | Uplink | S/C communications (4b) | 1963- |
| S | 2200-2290 | Downlink | S/C communications (5) | 1969-1973 |
| S | 2025-2100 | Uplink | S/C communications (5) | 1969-1973 |
| X | 8495 | up/down | Radar | 1974-1989 |
| | 8500-8520 | up/down | Radar | 1989-1999 |
| | 8500-8620 | up/down | Radar | 1999- |
| X | 8400-8450 | Downlink | S/C communications (4a) | 1973- |
| X | 7145-7190 | Uplink | S/C communications (4b) | 1973- |
| K | 22.0-22.3** | Down | SVLBI (2) | 1997-2005 |
| Ka | 31.8-32.3** | Downlink | S/C communications (4a) | 1998- |
| Ka | 34.2-34.7** | Uplink | S/C communications (4b) | 1998- |
| *DSN usage | ** GHz | | | |

(1) DSN support of the Soviet Venus Balloon Mission.
(2) DSN support of Space Very Long Baseline Interferometry (SVLBI) co-observing and radio astronomy observations.
(3) DSN 2388 MHz no longer instrumented and DSN 2320 MHz uplink authorization will be lost in the near future but reception from Arecibo at 2320 MHz will continue.
(4a) includes radio astronomy (web site: http//DSNra.jpl.nasa.gov/freq_man/index.html) and radio science,
(4b) includes radio science.
(5) DSN backup support of the near earth (less than 2x10^6 km) Apollo lunar manned space flight) missions.

Table 3-1 Tabulation of DSN frequencies used in accordance with the International Telecommunication Union (ITU) showing applications as a function of time.

### *3.4 Error correcting codes*

Deep space missions typically utilize binary phase shift keying (BPSK) modulation, in which bits are encoded as phase shifts applied to a RF carrier or sub-carrier signal. The rate of errors in detecting these BPSK-modulated bits is a function of the signal-to-noise ratio with which they are detected. In order to ensure that no more than 1 bit out of 100,000 is received in error (i.e., a bit error rate of $10^{-5}$) using uncoded BPSK modulation over a Gaussian communications channel, each bit must be received with a signal-to-noise ratio of 9.6 dB [see, for instance, Wozencraft, 1965].

Channel coding, or error correcting codes, can significantly reduce this SNR requirement, allowing higher data rates to be achieved with reduced communications system requirements. Error correcting codes work by transforming the original bit stream into a larger number of symbols with an algorithm that introduces intentional correlations among the symbols. The symbols are then transmitted, and those correlations allow some level of symbol errors at the receiving end to be detected and corrected. In 1959, Shannon showed that, in theory, codes exist that can provide error-free communications over an unconstrained bandwidth, Gaussian noise channel with a bit signal-to-noise ratio of only −1.6 dB or greater [Shannon, 1959]. Over the history of deep space communications, researchers have searched for actual code implementations that move us from the uncoded case progressively closer and closer to Shannon's limit.

The Pioneer 10/11 missions in the early 1970s utilized a constraint length 32, rate 1/2 convolutional code, reducing the required bit SNR from 9.6 to 7.1 dB. In a convolutional code of constraint length L and rate R, each bit in the original bit stream is converted into 1/R code symbols using an algorithm which is a function solely of the last L bits. The Viking missions, launched in the mid-1970s, employed a Reed-Mueller (32,6) block code, in which each block of six bits is coded as a 32-bit code word. This code reduces the bit SNR requirement to 6.0 dB. The Voyager missions, launched in 1977, combined these two types of coding, by concatenating an outer Reed-Solomon block code with inner (7,1/2) convolutional code, greatly reducing the required bit SNR to 2.4 dB. And by replacing the inner code with a more powerful (15, 1/6) convolutional code, we arrive at today's highest performance DSN code, with a bit SNR requirement of only 0.6 dB. Table 3-2 summarizes these codes, including a new class of turbo codes which we will discuss in section 5.

The value and importance of these coding advances can not be overstated. These coding schemes have offered roughly an order-of-magnitude increase in deep space communications capability. To achieve this same increase by simply replicating the existing assets of the current DSN ten times would represent a multi billion-dollar investment. Hence coding has provided an extremely cost-effective route to increased deep space communications performance.

Table 3-2: DSN decoding capability versus date, assuming a $10^{-5}$ BER.

| Code | Bit SNR, dB | Decoding | Mission (time period) |
|---|---|---|---|
| (32,1/2) [a] | 7.1 | Sequential | Pioneers 10/11 (1972-1974) |
| Reed-Mueller (32,6) | 6.0 | Block decoding | Vikings 1/2 (1975-1976) |
| (7,1/2), [a] Reed-Solomon (255,223) | 2.4 | Concatenated [b] | Voyagers (1977-1989) |
| (15,1/6), [a] Reed-Solomon (255,223) | 0.6 | Concatenated [b] | Cassini (1990-2000) |
| Turbo codes | -0.2 | Turbo decoding | (2001-beyond) |

[a] Convolutional code.

b Concatenated Viterbi and Reed-Solomon decoding.

In summary, there has been a substantial steady progression of DSN performance improvements from the early Pioneer missions to the present time. The resultant increased mission data rates are primarily due to technical improvements in the antennas performance, the lower LNA noise temperatures, improved coding techniques and migration to higher frequencies.

# 4. Deep Space Communications Today

The developments described in Section 3 have led to today's deep space communications capability. In this section we summarize the current state of the art of flight and ground deep space systems.

## *4.1 Summary of DSN antennas and their capabilities*

Today's DSN deep space antenna inventory consists of 12 operational antennas with capabilities at both S-and X-bands. These antennas consist of two standard (STD) 34m polar mount antennas, three High Efficiency (HEF) 34 m diameter az-el mount antennas, four beam waveguide (BWG) 34 m diameter az-el mount antennas and three 70 m diameter az-el mount antennas as shown in Fig. 4-1. (Fig. 4-1 also shows other antennas used for near earth applications such as launch support and Space Very Long Baseline Interferometry (SVLBI) as well as the signal processing centers.)

**DSN Facilities**

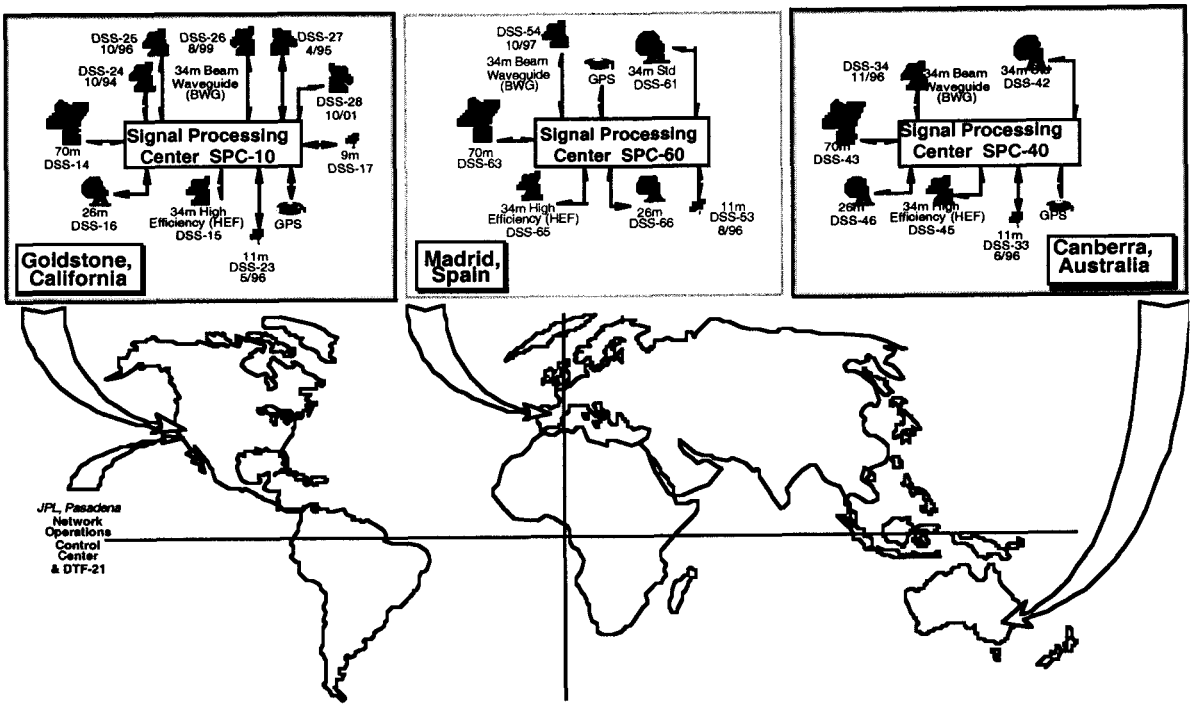

Fig. 4-1. Diagram of the current Goldstone, Madrid and Canberra DSN facilities including the deep space antennas as well as other antennas used for near earth applications such as launch support and Space Very Long Baseline Interferometry (SVLBI)

The key transmit and receive figures of merit for the DSN's operational antennas are shown in Table 4-1 [DSN Document 810-5]. Transmit performance is characterized by the product of antenna gain and transmitter power, while receive performance scales with the ratio of aperture effective area to system noise temperature. Items worthy of note include:

- The 70m antennas provide a unique worldwide high-power S-band uplink capability with an Equivalent Isotropic Radiated Power (EIRP) of 148 dBm. This has been an important resource in handling spacecraft emergencies, when it is critical to be able to uplink commands to a spacecraft which may be unable to point its high gain antenna to Earth. As missions move to X-band uplinks, plans are in place for adding X-band uplink capability to the 70m subnet over the next few years.
- An exceptionally low-noise receive system, known as an "ultracone", has been implemented on the Canberra 70m antenna to maximize data return from the southern-declination Galileo mission. By cryogenically cooling the feed components and minimizing waveguide elements, this maser-based system achieves a remarkable low system noise temperature of under 12 K at zenith in clear weather conditions.
- In addition to the S- and X-band downlink support capabilities, Table 4-1 also lists the first operational Ka-band (32 GHz) receive capability in the DSN, sited at the Goldstone DSS 25 BWG antenna. We will address the migration of deep space communications to this higher frequency in section 5.

Table 4-1: Performance parameters of the DSN's currently operational deep space communications antennas

| Antenna | Diameter | Transmit | | | Receive | | |
|---|---|---|---|---|---|---|---|
| | | Band | Ant Gain, dBi | Tx Power, kW | Band | Ant Gain, dBi | Tsys, K |
| ***Goldstone Deep Space Communications Complex*** | | | | | | | |
| DSS 14 | 70m | S | 62.7 (a) | 400 | S<br>X | 63.3 (d)<br>74.2 (d) | 15.2 (b)<br>20.6 (b) |
| DSS 15 | 34m (HEF) | X | 67.1 (a) | 20 | S<br>X | 56.0 (d)<br>68.3 (d) | 38.0 (b)<br>19.7 (b) |
| DSS 24 | 34m (BWG) | S | 56.1 (a) | 17.0 | S<br>X | 56.7 (d)<br>68.0 (d) | 30.2 (b)<br>25.4 (b) |
| DSS 25 | 34m (BWG) | X | 66.9 (a) | 3.6 | X<br>Ka | 68.1 (d)<br>78.6 (d) | 23.4 (b)<br>46.9 (b) |
| DSS 26 (e) | 34m (BWG) | X | 66.9 (a) | 3.6 | X | 68.1 (d) | 29.7 (b) |
| *Canberra Deep Space Communications Complex* | | | | | | | |
| DSS 42 | 34m (STD) | S | 55.2 (a) | 20 | S<br>X | 56.2 (d)<br>66.2 (d) | 21.5 (b)<br>25.4 (b) |
| DSS 43 | 70m | S | 62.7 (a) | 400 | S<br>X | 63.3 (d)<br>74.2 (d) | 11.7 (b,c)<br>21.0 (b) |
| DSS 45 | 34m (HEF) | X | 67.1 (a) | 20 | S<br>X | 56.0 (b)<br>68.3 (b) | 38.0 (b)<br>20.1 (b) |
| DSS 34 | 34m (BWG) | S<br>X | 56.1 (a)<br>66.9 (a) | 17.0<br>3.6 | S<br>X | 56.7 (d)<br>68.0 (d) | 29.4 (b)<br>30.0 (b) |
| ***Madrid Deep Space Communications Complex*** | | | | | | | |
| DSS 61 | 34m (STD) | S | 55.2 (a) | 20 | S<br>X | 56.2 (d)<br>66.2 (d) | 21.5 (b)<br>25.4 (b) |
| DSS 63 | 70m | S | 62.7 (a) | 400 | S<br>X | 63.3 (d)<br>74.2 (d) | 16.9 (b)<br>21.0 (b) |
| DSS 65 | 34m (HEF) | X | 67.1 (a) | 20 | S<br>X | 56.0 (b)<br>68.3 (b) | 42.0 (b)<br>20.1 (b) |
| DSS 54 | 34m (BWG) | S<br>X | 56.1 (a)<br>66.9 (a) | 17.0<br>3.6 | S<br>X | 56.7 (d)<br>68.0 (d) | 29.4 (b)<br>23.8 (b) |

(a) at gain set (optimized) elevation angle, no atmosphere included
(b) referenced to LNA input, average clear weather, zenith, non-diplexed low-noise path
(c) ultracone
(d) at gain set elevation angle, average clear weather
(e) slated for operation after year 2000

## *4.2 Current Spacecraft Communications Systems: Two Views*

Deep space exploration is completing an important period of transition from large, expensive, infrequent, but highly sophisticated "flagship" missions to much more frequent, smaller, lower-cost, focused science missions. Here we examine two spacecraft systems, representing each of these mission classes.

### 4.2.1 Cassini

The Cassini spacecraft carries the most sophisticated radio system ever flown in deep space. Launched on October 15, 1997, Cassini will arrive at Saturn in July, 2004. Figure 4-2 shows the major components of the Cassini spacecraft. The 5634 kg spacecraft carries a wide range of science instruments, including IR, optical, and UV imagers, microwave remote sensing systems, fields and particles instruments, and interdisciplinary science experiments. The scientific goals of the Cassini mission pose a number of communications challenges:

- This first extended tour of the Saturnian system (as opposed to the brief flybys of Saturn by Voyager 1 in November, 1980 and Voyager 2 in August, 1981) will generate large data volumes to be returned from the outer solar system at large distances of about

10 AU. (One Astronomical Unit [AU], defined as the radius of the Earth's orbit about the sun, is approximately 150 million kilometers.)

- The Cassini spacecraft carries the Huygens probe, which will be dropped into the atmosphere of Saturn's moon Titan. The primary Cassini spacecraft must act as a relay for the telemetry generated by the Huygens probe.
- In addition to its communications function, the radio signal will also serve as a science instrument for a variety of investigations, including Saturn ring occultations as well as the most sensitive search to date for long-wavelength gravitational radiation.

Cassini's deep space telecommunications needs are supported by a 4-m multi-frequency high-gain antenna, redundant 19-W X-band Traveling Wave Tube Amplifiers (TWTAs), and redundant X-up/X-down Deep Space Transponders with accompanying command and telemetry processing systems. Table 4-2 lists key parameters of the Cassini radio system. The high-gain antenna, supplied by the Italian Space Agency, operates at X-band for telecommunications, but also at S, Ku, and Ka-bands for various science functions. A pair of low-gain antennas provide for emergency communications and for low-rate communications during cruise when the body-fixed high-gain antenna is not pointed towards Earth. In addition to the X/X communications transponder, the spacecraft also provides for X-up/Ka-down and Ka-up/Ka-down frequency translation to support the radio science experiments. The higher-frequency Ka-band links significantly reduce charged particles scintillation effects due to solar plasma and the Earth's ionosphere, enabling Doppler measurement sensitivities of $3 \times 10^{-15}$.

Table 4-2 Cassini Radio Frequency System

| **Element** | **Features** | **Mass, kg** | **DC Power,W** |
|---|---|---|---|
| Deep Space Transponder | X-up/X-down; -157 dBm carrier tracking threshold | 2 x 8.6 | 20.2 |
| X-band TWTA | 20 W RF output | 2 x 5.4 | 57.1 |
| High-gain Antenna | 4 m diameter, 46 dBi gain | 100 | - |
| Low-Gain Antennas | | 1.4 | - |
| Ultra Stable Oscillator | High-stability reference for low-SNR downlink telemetry and radio science | 1.8 | 2.8 |
| Diplexers, waveguide switches, coax and misc hardware | | 15.3 | - |
| Total RFS | | 146.5 | 80.1 |

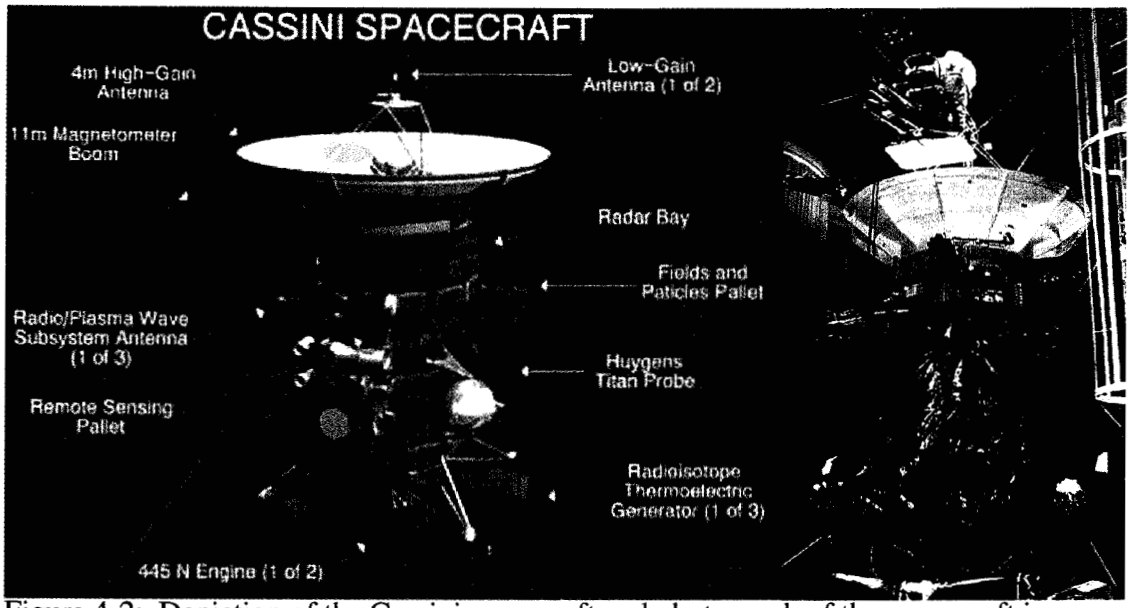


Figure 4-2: Depiction of the Cassini spacecraft and photograph of the spacecraft in environmental test.

### 4.2.2 Mars Pathfinder

During the Cassini development phase, NASA turned towards a new "faster-better-cheaper" approach to solar system exploration, based on much more frequent launches of smaller, lower-cost spacecraft with focused science objectives. NASA established the Discovery Program to begin to carry out this new class of exploration, and the Mars Pathfinder mission represents one of the first missions in this Discovery Program. A primary goal of Mars Pathfinder was to demonstrate the technical feasibility of landing safely on the surface of Mars, within the programmatic constraints of a $150M mission cost cap and 3-year development cycle. Compared to the 5634 kg mass of the Cassini spacecraft, the Pathfinder spacecraft launch mass, including propellant, was only 890 kg. Mars Pathfinder launched from the Kennedy Space Center on December 4, 1996, arriving at Mars on the 4$^{th}$ of July, 1997.

Key elements of the Mars Pathfinder Radio Frequency Subsystem are listed in Table 4-3. Pathfinder flew a copy of the same Deep Space Transponder that was developed and flown on Cassini. But, reflecting the lower-cost, higher-risk philosophy of the Discovery program, Pathfinder flew a single string system with a single transponder and power amplifier. Pathfinder also flew a lower-mass, lower-cost Solid-State Power Amplifer in place of the Cassini TWTA, and Pathfinder's high-gain antenna was a compact 11" diameter array antenna, with two orders of magnitude less X-band gain that the 4m Cassini antenna.

As a result, in spite of the closer proximity to Earth, Pathfinder's high-gain link typically supported data rates of only up to 8 kbps. Transmission time from the surface was also limited to only a few hours per Mars sol (a sol is a single 25-hr Mars day) due to solar-collected energy constraints onboard the Pathfinder lander. Over the entire 83 sol duration of the lander mission, a total of 2.3 Gbits of data were returned, corresponding to an average of about 30 Mb/sol. The bulk of this data volume was used to transmit 16,500 lander images and 550 rover images from the Martian surface.

Table 4-4 provides a comparison of the key spacecraft parameters of Cassini and Pathfinder.

Fig. 4-3: The Mars Pathfinder lander, on the surface of Mars, as imaged by the Sojourner rover.

Table 4-3 Mars Pathfinder Radio Frequency Subsystem

| Element | Features | Mass, kg | DC Power, W |
|---|---|---|---|
| Deep Space Transponder | X-up/X-down; -157 dBm carrier tracking threshold | 4.9 | 11.0 |
| X-band SSPA | 13 W RF output | 1.7 | 57.0 |
| High-gain Antenna | 11" diameter printed dipole array, 23.6 dBi transmit gain | 1.2 | - |
| Low-Gain Antennas | | 1.1 | - |
| Diplexer, waveguide switches, coax and misc hardware | | 1.1 | - |
| Total RFS | | 10.0 | 68.0 |

Table 4-4: Comparison of Cassini and Mars Pathfinder Telecom Characteristics

| Item | Cassini | Mars Pathfinder |
|---|---|---|
| Radio System Mass, kg | 146.5 | 10.0 |
| Radio System DC Power, W | 80.1 | 68.0 |
| EIRP, dBm | 89 | 65 |
| Maximum downlink data rate, kbps | 100 (from Saturn, to 70m DSN antenna) | 8 (from Mars, to 70m DSN antenna) |

## 5. Future Directions

While the development of deep space communications over the past 50 years represents an

impressive technical accomplishment, it is clear that we have a long way to go before we truly achieve NASA's goal of creating a virtual presence throughout the solar system. Pathfinder gave us a glimpse of the scientific and public excitement that results from extended in situ presence on another planet in our solar system. And yet the Sojourner rover only explored a tiny region around the Pathfinder lander. The Pathfinder link to Earth, with a maximum data rate of 8 kbps and connectivity of just a few hours per day, is a far cry from the type of Internet access we take for granted in our homes and offices. And our planetary missions typically utilize data rates many orders of magnitude less than the data rates of Earth-orbiting scientific missions, severely constraining the types of instruments we can fly and the resolution with which we can globally map bodies in our solar system.

Achieving a meaningful virtual presence will call for a second era of deep space communications development. This era will establish breakthrough increases in bandwidth and connectivity between Earth and robotic explorers throughout the solar system. While past deep space missions traditionally represented single point-to-point links between a planetary spacecraft and Earth, the future calls for more complex network topologies, with *in situ* exploration involving landers and rovers communicating through networks of relay satellites. The future will demand a layered deep space network architecture that supports infusion of "physical layer" technology advances to increase communications performance while supporting higher-level information management such as file transfers over deep space links.

The trend to much lower-cost missions is allowing NASA to fly many more simultaneous missions than at any time in its history. This increased mission set, along with the high data volumes represented by orbital mapping and in situ investigations, as well as the interest in exploring distant outer planet targets like Europa, Neptune, and Pluto, will further drive the demand for increased communications capacity of the Deep Space Network. This section examines some of the technologies that will help meet these demands.

### *5.1 Ka-band Ground Systems*

As a first step towards increasing the agency's deep space communications capacity, NASA's Deep Space Network (DSN) is initiating the implementation of Ka-band (32 GHz) reception capabilities on all of its ground assets [Edwards, et al., 1998]. Currently, most deep space missions utilize X-band (8.4-GHz) communications links for telemetering data back to Earth. Recalling the link equation in Section 1, we see that moving to higher frequencies is an effective way to increase communications performance, without increasing the spacecraft transmitted power or the spacecraft and ground aperture size. The performance improvement results from the fact that, for a given antenna size, moving to the higher Ka-band frequency focuses the downlink radio signal into a narrower beam, increasing the power received over a given aperture on Earth. After accounting for the increased impact of the atmosphere at Ka-band, and the lower efficiency of some of the transmit and receive elements, we expect an overall increase of roughly 6 dB, by moving from X-band to Ka-band.

Achieving adequate aperture efficiency with the DSN'S large aperture antennas at the short sub-cm wavelength of Ka-band represents a significant challenge. Gravity-induced deformations in the primary antenna surface, as the primary antenna tips in elevation, can lead to large losses in efficiency. While the DSN's new 34m Beam WaveGuide (BWG) antennas were specifically designed with stiff structures to minimize these deformations,

providing excellent aperture efficiency (50-60%) over the full range of elevation angles, the older 70m antennas suffer very large gravity-induced deformations that, if left uncorrected, would preclude their use at Ka-band. Researchers at JPL are currently investigating two techniques for compensating these deformations and obtaining high aperture efficiency on the 70m antennas (Figure 5-1). The first technique, called a Deformable Flat Plate, places a small reflector with 21 actuators distributed across its face in front of the Ka-band feed system on the 70m antenna. The actuators are programmed to deform this mirror, as a function of elevation angle, to exactly compensate for the predicted gravity-induced deformations of the large 70m primary dish. The second technique, called an Array Feed, surrounds a central Ka-band feed with six additional feeds in a hexagonal pattern. These outer feeds capture the energy in the defocused beam caused by the primary antenna deformation. Real-time signal processing determines the relative phase and amplitude of the signal in each feed element. Based on these complex weights, the seven feed signals are recombined in an adaptive way to compensate for the gravity distortion. Both of these systems are currently being tested on the Goldstone 70m antenna, in order to quantity potential future 70m Ka-band performance and determine a recommended implementation approach.

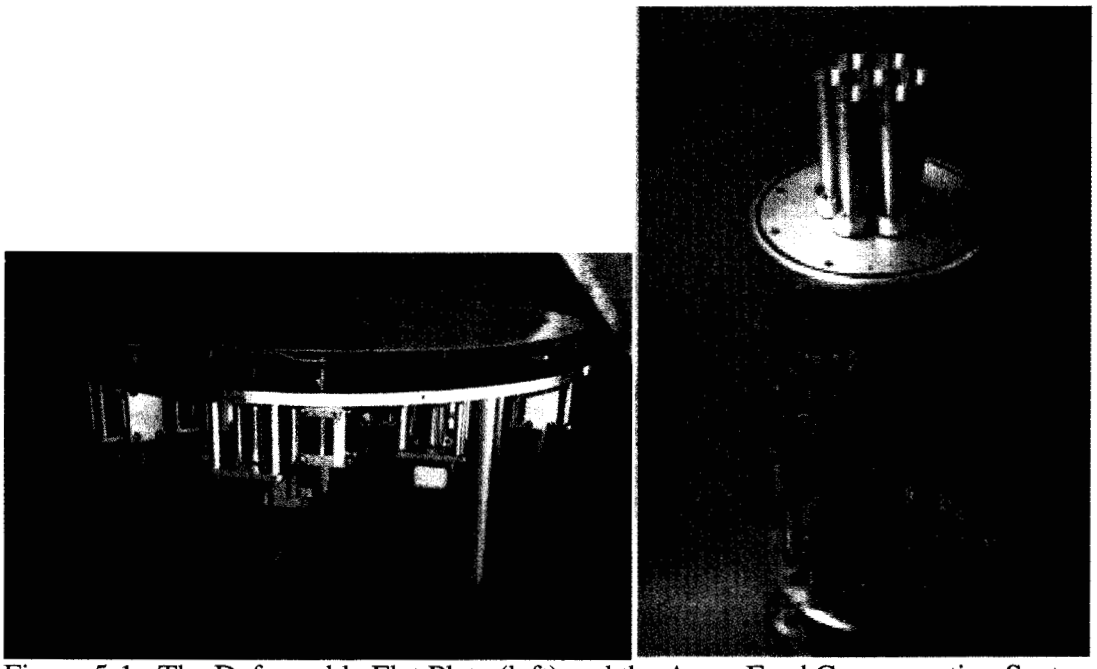

Figure 5-1: The Deformable Flat Plate (left) and the Array Feed Compensation System (right), two candidate technologies for implementing Ka-band telemetry capability on the DSN's 70m subnet.

Accurate pointing is another challenge of operating at Ka-band, since the antenna beamwidth is four times smaller than at X-band. A new feed has been developed that provides X-band transmit and receive capability, along with a tracking Ka-band receive capability, all in a single aperture [Stanton, et al., 1997]. This feed can provide closed-loop Ka-band antenna pointing to better than a millidegree of accuracy. This feed can be used by itself on a 34m antenna, or can be combined with the Deformable Flat Plate on the 70m to provide gravity compensation and closed-loop pointing. The Array Feed system, on the other hand, intrinsically provides pointing information in addition to gravity compensation based on the spatial distribution of energy across its seven array elements.

A final key technology for Ka-band ground systems are the low-noise amplifiers that provide high-sensitivity signal reception. Recent developments with cryogenic Indium Phosphide (InP) High Electron Mobility Transistor (HEMT) amplifiers have achieved amplifier module noise temperatures of less than 10 K. Even lower noise temperatures can be obtained with maser-based amplifier systems at Ka-band [Shell, et al., 1994]. With these cryogenic low-noise systems, total system noise temperatures at 32 GHz become dominated by atmospheric emissions, which are significantly higher at Ka-band than at X-band. As a result, the DSN has collected several years of atmospheric brightness temperature statistics at all three complexes to provide accurate Ka-band weather models [Morabito, et al., 1998].

To assess the end-to-end performance of Ka-band deep space telecommunications, several flight demonstrations have been conducted. Launched on September 25, 1992, the Mars Observer spacecraft transmitted the first deep space Ka-band signal, which was successfully received at the DSS 13 34m BWG research and development antenna at the Goldstone tracking complex. Although the Mars Observer Ka-band Link Experiment (KaBLE) was limited to a very low transmitted power and small transmit aperture, the experiment successfully demonstrated reception of the transmitted Ka-band carrier, telemetry, and ranging signal. It also validated Ka-band atmospheric models and served as a testbed for many of the ground system component technologies required for good 34m and, ultimately, 70m aperture performance at 32 GHz. Subsequent to the loss of the Mars Observer spacecraft in August, 1993, a second Ka-band Link Experiment was developed and launched on the Mars Global Surveyor spacecraft on November 7, 1996. Relative to the original Mars Observer KaBLE experiment, the KaBLE-II experiment increased the Ka-band EIRP by 26 dB, through the flight of a 1W Ka-band SSPA and use of the entire 1.5-meter MGS high gain antenna. Finally, the New Millennium DS1 experiment carries a Ka-band flight demonstration, including the first commercially-available Ka-band-equipped deep space transponder (the Small Deep Space Transponder, built by Motorola under contract to JPL). Both MGS and DS1 are currently being used to quantify the Ka-band performance of DSS25, the DSN's first operational Ka-band antenna.

The DSN is currently initiating a Ka-band development roadmap that calls for the addition of Ka-band feeds to all five operational BWG antennas by 2003, followed by implementation of Ka-band on the 70m and 34m HEF antennas later in the decade. When this evolution is complete, the deep space communications capacity of the DSN will have been increased by roughly 6 dB over its current X-band capability, for a given spacecraft DC power and antenna size, due to the higher directivity of the Ka-band signal. Compared to the cost of increasing the number of antennas in the DSN, the addition of Ka-band capabilities to the existing DSN apertures is an extremely cost-effective means of increasing deep space communications capacity for NASA's future mission set.

### *5.2 Spacecraft Radio Systems*

New spacecraft radio system elements are required to enable future Ka-band missions. Key drivers on these elements are low mass and power, high efficiency, high EIRP, and low cost. At the heart of the future radio system is the Spacecraft Transponding Modem (STM) [Riley, et al., 1996]. The STM provides X-band receiver and X/Ka-band exciter functions, supports new high-performance turbo codes, presents a simple frame-level interface to the flight computer, and provides timing and frequency references for the entire spacecraft, all in a 0.9-kg package that consumes less that 11 W. A full prototype of the STM is currently under development, with completion targeted for 2000.

A critical need for effective use of Ka-band is high-efficiency spacecraft power amplifiers. Current solid-state amplifiers are limited by low output power and efficiency; for example,

the Ka-band SSPA on the New Millennium DS1 mission provides about 2.5 W of RF power with only about 15% DC-to-RF power efficiency. In the near term, Travelling Wave Tube Amplifiers provide a path to much higher output power and efficiency. Design goals for a 32 GHz TWTA being developed for NASA missions in the 2003-2005 time frame include an output power of 15-30 W, efficiency of greater than 40%, and mass of under 2 kg. In the longer term, improvements in solid state devices, coupled with quasi-optic combining techniques to allow combining output from multiple devices without the inherent losses of microstrip combining, will open the door to low-mass, low-cost Ka-band solid state amplifiers with comparable performance specifications.

In addition to improved power amplifiers, new spacecraft antenna designs provide a path to higher levels of spacecraft EIRP. The migration to Ka-band frequencies for conventional fixed Cassegrain reflectors is well in hand with the successful Mars Global Surveyor Ka-band Link Experiment, which achieved a gain of 49.0 dBi with the 1.5 m high gain antenna at 32 GHz [Butman, et al., 1997]. And the Cassini spacecraft's 4 m antenna will support Ka-band radio science investigations with a 32 GHz antenna gain of 59 dBi. However, the trend towards low-cost spacecraft and smaller launch vehicles typically constrains future fixed spacecraft antennas to diameters of under 2 m. As a result, there is renewed interest in deployable large-aperture antennas which can launch with a small stowed volume [Freeland, et al., 1998a,b]. The IN-STEP Inflatable Antenna Experiment (IAE), which flew on the Space Shuttle mission STS-77 in 1996, successfully demonstrated the feasibility of deploying a large, 14-m diameter inflatable structure in space.
While the IAE did not include on-orbit RF characterization of the deployed reflector, the IAE structure itself was manufactured with a surface tolerance of 2 mm. This level of surface tolerance can provide good X-band performance; further improvements to better than 1 mm will enable Ka-band applications.

Reflectarray antennas provide another interesting approach to spacecraft apertures. With this technique, a flat surface (or in fact any surface shape) is illuminated with an RF signal, and reflecting patch elements on the surface reflect the RF signal. By properly designing the phase delay of each patch element, the surface can be made to emulate a parabolic reflector over a limited frequency range. This approach can enable multifunctional spacecraft structural surfaces which can also serve as high gain antenna reflectors. A 0.5-m prototype Ka-band reflector has been developed, achieving aperture efficiency of 60% [Huang, et al., 1998]. And more recently, as shown in Figure 5-2, reflectarray and inflatable antenna concepts are being merged, with the development of a prototype 1m inflatable antenna, with a mass of only 1.2 kg, in which the inflatable struts stretch a thin membrane covered with reflectarray patches [Huang, et al., 1999]. A larger 3m inflatable reflectarray supporting Ka-band operation is currently in development. Based on the low areal density and small stowed volume of these inflatable antennas, this technology represents a potential breakthrough in RF-based deep space communications.

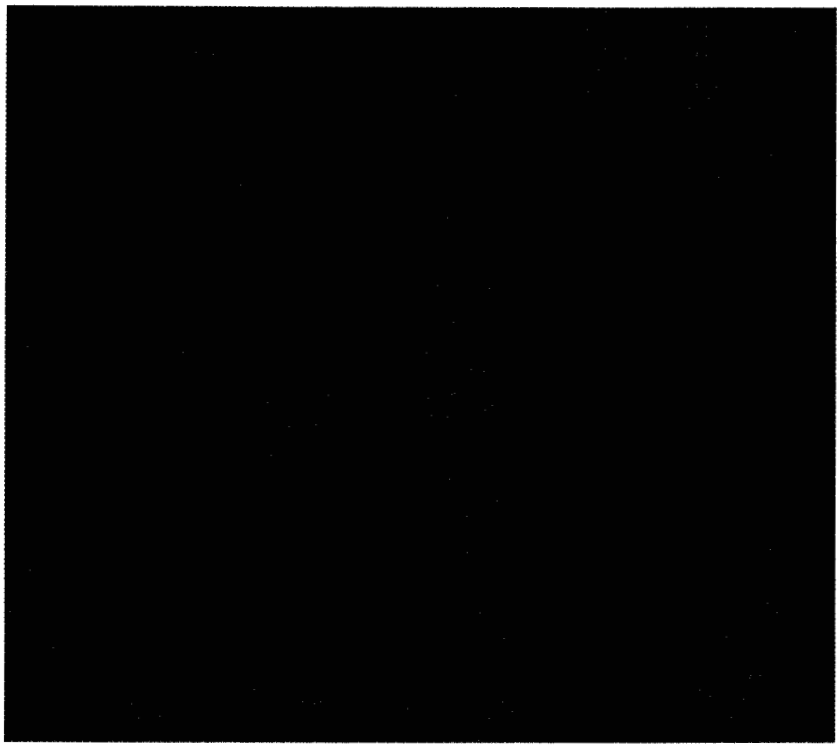

*Figure 5-2: 1m X-band Inflatable Reflectarray prototype antenna*

### 5.3 Optical Communications

Moving beyond Ka-band, communication at optical wavelengths offers even further opportunities for performance improvements, again based on the higher directivity of the spacecraft signal as wavelength decreases. For instance, a diffraction limited 2-meter Ka-band antenna transmits its signal with a beamwidth of about 5 millirad. By contrast, an optical (1064 nanometer) spacecraft laser transmitted through a much smaller 30 cm diffraction-limited telescope has a beamwidth of just 3.5 microradians. This represents more than a million-fold increase in transmit aperture gain.

A prototype spacecraft optical transceiver, suitable for deep space applications as well as high-rate near-earth missions, has been developed at JPL [Chen, et al.; 1994, Yan, et al., 1997]. The Optical Communications Demonstrator (OCD) utilizes a simple architecture with a single detector array and just one fine steering mirror providing acquisition and tracking of an uplink beacon signal, transmit beam pointing, and transmit/receive relative beam positioning to accommodate point-ahead angles due to relative cross-velocity. The OCD includes a 10-cm transmit receive optics, a fiber-coupled transmit laser, and a separate control processor, with a total mass of 8 kg and power of 30 W (Figure 5.3). The internal fine steering mirror handles vernier pointing, allowing the overall system to have relatively coarse pointing requirements.

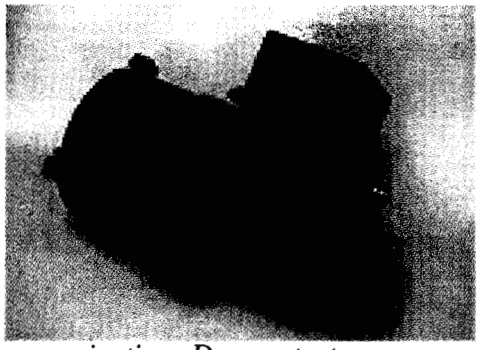

*Figure 5-3: The Optical Communications Demonstrator*

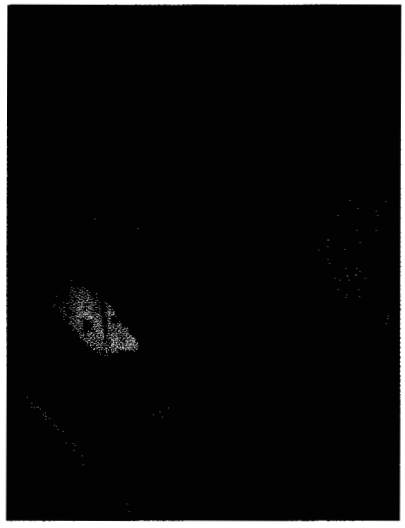

*Figure 5-4: Multi-beam laser uplink from Table Mountain 0.6m Telescope to the ETS-VI spacecraft during the Ground to Orbit Lasercom Demo (GOLD)*

Several important system-level demonstrations of optical communications have already been carried out. In December, 1992, a demonstration of uplink ground-to-space optical communications was successfully conducted with the Galileo spacecraft [Wilson, et al., 1993a; Wilson, et al., 1993b]. Uplink laser signals were transmitted from two ground telescopes: the Starfire Optical Range in New Mexico and the Table Mountain Observatory in southern California. The transmitted signal was successfully received using the Galileo science imaging camera at spacecraft ranges of up to $6 \times 10^6$ km.

A second optical communications space demonstration was carried out from November 1995 – May 1996 as a collaboration between JPL and the Communications Research Laboratory (part of the Japanese ministry of Telecommunications and Posts), as a cooperative effort between NASA and NASDA [Wilson, et al., 1997a; Wilson, et al., 1997b]. In this Ground-to-Orbit Lasercom Demonstration (GOLD) experiment, an optical signal was transmitted from the 0.6-m telescope at Table Mountain and received by the CRL optical communications transceiver on the ETS-VI spacecraft, which then transmitted a signal back to Earth to be received at the 1.2-m Table Mountain telescope. Data rates as high as 1 Mb/s were achieved on both the uplink and downlink. As shown in Figure 5-4, one of the important results of the GOLD experiment was the use of multiple uplink beams, spatially and temporally decorrelated, to significantly reduce the effects of atmospheric scintillation on the uplink signal.

In concert with these developments JPL has initiated the development of a 1-meter Optical Communications Telescope Laboratory (OCTL), sited at the Table Mountain Facility in southern California. This facility will support early earth-orbiting demonstrations of space-to-ground optical communications, such as the planned ISSERT demonstration on the International Space Station, scheduled for 2002. OCTL will also provide an R&D testbed for developing the ground system technologies that will ultimately be used for deep space optical communication applications. It is envisioned that a 1-meter uplink telescope, similar to OCTL, would be complemented by a larger, 10-meter class "photon bucket" - a non-diffraction-limited optical collector for receiving the downlink optical signal.

In the long term, optical communications offers the potential for significant advances in deep space communications bandwidth and reductions in spacecraft system mass and power. Based on current optical communications system design, a single 10m ground station supporting a downlink from a spacecraft at Jupiter equipped with a 3W, 30 cm optical transmitter could achieve roughly the same data rate as the equivalent performance of *all* of the DSN's current X-band antennas arrayed together, receiving a 10W X-band signal from a 1.5-meter spacecraft antenna. And it is expected that future component level improvements in optical detector and laser efficiencies, as well as improved optical modulation and coding schemes, will further increase these performance gains. NASA's current communications roadmap calls for technology development and demonstrations in the 2000-2005 time frame with OCTL, and the initial deployment of the first operational 10m ground station(s) in the 2008-2010 time frame. Looking beyond 2010, an important strategic decision is whether to continue the relatively low-cost development of optical ground stations, which must contend with significant atmospheric effects, or to move to Earth-orbiting assets to support deep space optical communications. Technology breakthroughs in low-cost spacecraft and lightweight optical system will play a key role in this decision.

### *5.4 Protocols, Coding and Data Compression*

The long round-trip light times, high bit error rates (compared to terrestrial fiber links), and intermittent link availability encountered in interplanetary communications are incompatible with current Internet Protocol (IP) standards. NASA is developing new standards which represent a natural evolution of IP functionality to the deep space environment. The CCSDS File Delivery Protocol (CFDP), currently in development, will provide for reliable and robust file delivery from in situ vehicles back to Earth, even through multiple, intermittent relay communications assets [CCSDS, 1999].

New classes of error correcting codes, known as turbo codes, are being developed which will increase data communications rates achievable for a given spacecraft radio system [Divsalar, et al., 1995]. These codes offer 2 dB better performance than the standard (7,1/2) convolutional code, and nearly 1 dB better than the newer (15,1/6) code, and the lower decoder complexity allows the use of these codes at higher bit rates. The DSN is planning to implement an operational turbo decoding capability by 2003.

In spite of all of these communications-enhancing technologies, for deep space missions we will always be working in a regime in which the available data rates back to Earth are small compared to terrestrial capabilities we take for granted, and compared to the raw data rates of advanced multispectral sensors. Maximizing the *information* that we can convey on this bandwidth-constrained link will require aggressive use of data compression. New lossless and lossy data compression techniques are being developed for use in the Mars Surveyor Program and other deep space missions. Beyond conventional data

compression, concepts like progressive transmission and onboard data mining will be used to extract data subsets of highest science value for transmission to Earth. In progressive transmission, a science dataset is coded and transmitted in a manner that first delivers a low-resolution representation of the data; ground-based scientists can then evaluate this low-resolution version and, if warrented, request transmission of additional data to progressively refine the resolution. In onboard data mining, science processing algorithms are carried out onboard the spacecraft to discover particular datasets of high scientific interest for transmission to Earth. Both of these techniques are aimed at maximizing the science information that can be communicated over a severely bandwidth-constrained deep space link.

### *5.5 A Mars Network for Telecommunications and Navigation*

Mars represents a near-term objective where many of these future technologies can come together to establish the first step towards an Interplanetary Internet. NASA has recently completed a comprehensive study of the overall architecture of Mars exploration in the time frame through 2011, including robotic sample return missions, precursor missions for human exploration, and a wide range of low-cost science micromissions. In the context of this study, the enhancing and enabling aspects of a Mars Network, providing increased telecommunications and navigation capabilities, were recognized. Pathfinder-era capabilities of 30 Mb/sol data return and few-hours/sol link connectivity represent a fundamental barrier to increasingly sophisticated Mars in situ exploration. Two conceptual building blocks for an evolving Mars Network were identified during the study. The first is a very low-cost microsatellite, which would be launched as a piggyback payload on a commercial Ariane launch into geosynchronous transfer orbit. The 200-kg microsatellite would then park in an Earth-moon orbit until the optimal time for transfer to Mars. A constellation of these satellites would be established in low altitude (400-1000 km) Mars orbits, providing high-sensitivity UHF relay capabilities, frequent telecommunication contacts, and GPS-like navigation services to surface assets. A constellation of six such satellites could provide multi-Gb/sol data return with dozens of contacts per sol.

The second building block is called the Mars Areostationary Relay Satellite (MARSAT), and would orbit Mars at an altitude of 17,000 km in a circular, equatorial orbit with a period of 1 sol; i.e., the Martian equivalent of a Earth geostationary satellite. Using high-gain links at X-band or Ku-band between the surface and MARSAT, and a 100 W Ka-band link back to Earth, MARSAT would provide nearly continuous 1 Mb/s data rates from the surface of Mars back to Earth, supporting streaming video imagery (or other high data rate information) from in situ spacecraft to scientists and the public on Earth. This quantum leap in bandwidth and connectivity would fundamentally change our science mission operations concepts and open exciting new doors in how NASA can engage the public in the excitement of Mars exploration (Figure 5-5).

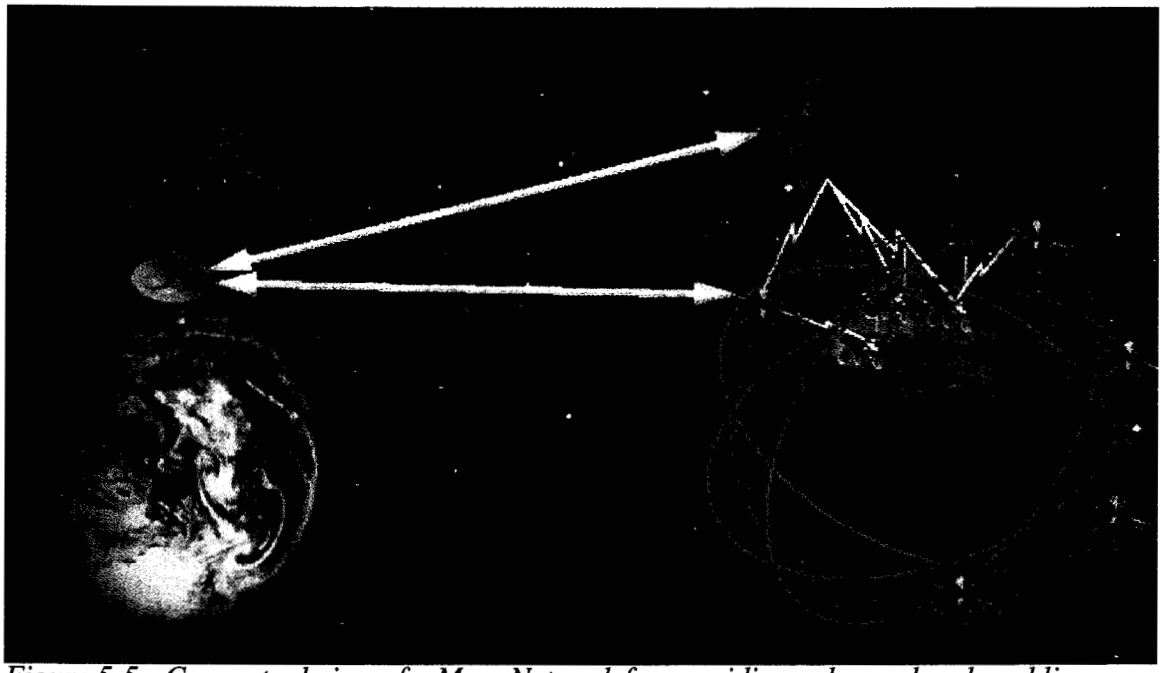

*Figure 5-5: Conceptual view of a Mars Network for providing enhanced and enabling telecommunications and navigation capability for future robotic and human mission to Mars.*

## 6. Summary

Over the last half of the 20th century, advances in flight and ground radio system technologies have provided a remarkable growth in NASA's ability to bring high-rate science data back from the furthest reaches of the solar system. The large apertures and sensitive low-noise receivers of NASA's Deep Space Network, coupled with high-gain spacecraft antennas, efficient spacecraft power amplifiers, increased carrier frequencies, and innovative channel coding schemes, have all contributed to this growth.

The coming millennium will demand continued growth in communications capability to support the agency's goal of establishing a virtual presence throughout the solar system. This communications growth must be accomplished in an era of small, low-cost spacecraft. This challenge will be met by further increases in communications frequency, first to Ka-band, and ultimately to laser-based optical communications. The vision of an Interplanetary Internet, which will layer efficient deep space communications protocols on top of this evolving physical link layer, will redefine the way in which future missions will move information across the solar system. And fifty years from now, NASA may well be embarking on missions beyond our own solar system, targeting neighboring stars about which we may have detected planetary systems, and driving the need for yet another era of communications advances.

## 7. Acknowledgements

The work described was performed at the Jet Propulsion Laboratory, California Institute of Technology under contract with the National Aeronautics and Space Administration.

## 8. References

CCSDS File Delivery Protocol (CFDP), Red Book, 727.0-R-2., http://www.ccsds.org/ccsds/internal/pubs/RP9902/index.html, March 1999.

C.-C. Chen and J. R. Lesh, Overview of the Optical Communications Demonstrator, in : *Proc. Of SPIE OE/Lase 94,* Paper #2123-09, Los Angeles, CA, 1994.

R. C. Clauss and E. Wiebe,"Refrigerated Coaxial Coupling," U. S. Patent # 3,902,143, 1975.

R. C. Clauss and R. Quinn, "Resonant Isolator for Maser Amplifer," U. S. Patent # 4,399,415, 1983.

W. R. Corliss, "A History of the Deep Space Network," NASA CR-151915, May 1976.

Divsalar, D. and F. Pollara, "On the Design of Turbo Codes", The Telecommunications and Data Acquisition Progress Report 42-123, July-September 1995, November 15, 1995 (http://tmo.jpl.nasa.gov/tmo/progress_report/).

DSN Document 810-5, DSN/Flight Project Interface Design Handbook, available on-line at http://deepspace1.jpl.nasa.gov/dsndocs/810-5/810-5.html, Jet Propulsion Laboratory, California Institute of Technology, Pasadena, California.

C. D. Edwards, C.T. Stelzried, L.J. Deutsch, and L. Swanson "NASA's Deep Space Telecommunications Roadmap," The Telecommunications and Mission Operations Progress Report 42-136, February 15, 1999 (http://tmo.jpl.nasa.gov/tmo/progress_report/).

C.D\. Edwards, L.J. Deutsch, M. Gatti, J. Layland, J. Perret, and C. Stelzried, "The Status of Ka-band Communications for Future Deep Space Missions," Proceedings of the Third Ka Band Utilization Conference, pp 219-225, Sorrento, Italy, September 15-18, 1997.

Freeland, R. E; Bilyeu, GD; Veal, GR; Mikulas, MM, "Inflatable deployable space structures - Technology summary," IAF, International Astronautical Congress, 49th, Melbourne, Australia, Sept. 28-Oct. 2, 1998a.

Freeland, RE; Veal, GR, "Significance of the Inflatable Antenna Experiment technology," AIAA/ASME/ASCE/AHS/ASC Structures, Structural Dynamics, and Materials Conference and Exhibit, 39th, and AIAA/ASME/AHS Adaptive Structures Forum, Long Beach, CA, Apr. 20-23, 1998, Collection of Technical Papers. Pt. 4 (A98-25247 06-39), Reston, VA, American Institute of Aeronautics and Astronautics, Inc., 1998b, p. 2789-2796.

R. M. Goldstein, "Radar Time-of-Flight Measurments to Venus," Astron. J. August 1968.

W. H. Higa and E. Wiebe, ""A Simplied Approach to Heat Exchanger Construction for Cryogenic Refrigerators," Cryogenic Technology, March/April 1967.

Howard, H. T., et al, "Mercury: Results on Mass, Radius, Ionosphere, and Atosphere from Mariner 10 Dual-frequency Radio Signals," Science, July 1994.

Huang, J. and R. J. Pogorzelski, "A Ka-band microstrip reflectarray with elements having variable rotation angles", IEEE Transactions on Antennas & Propagation, Vol. 46. May 1998.

Huang, J. and A. Feria, "A 1-m X-band inflatable reflectarray antenna", Microwave and Optical Technology Letters, Vol. 20, No. 2, Jan. 20, 1999.

R. M. Jaffee and E. Rechtin, "Design and Performance of Phase-Locked Circuits Capable of Near-Optimum Performance Over a Wide Range of Input Signals and Noise Levels," IRE Transactions on Information Theory, March 1955.

C. R. Koppes, "JPL and the American Space Program," Yale University Press, 1982.

J.W. Layland and D.W. Brown, "Planning for VLA/DSN Arrayed Support to the Voyager at Neptune," JPL TDA PR 42-82, August 1985.

G. S. Levy, et al, "The Ultra Cone: An Ultra Low-Noise Space Communication Ground Radio-Frequency System," MTT Special Issue on Noise, MTT-16, September 1968.

K. W. Linnes, W.D. Merrick and R. Stevens, "Ground Antenna for Space Communication System," IRE Transacations on Space Electronics and Telemetry," March 1960.

Lo, V. Y., "Ka-Band Monopulse Antenna-Pointing Systems Analysis and Simulation", The Telecommunications and Data Acquisition Progress Report 42-124, October-December 1995, February 15, 1996 (http://tda.jpl.nasa.gov/tda/progress_report/).

W. H. Michael, et al, "The Viking Radio Science Investigations," Journal of Geophysical Research, September 1977.

Morabito, D., R. Clauss, and M. Speranza, "Ka-Band Atmospheric Noise-Temperature Measurements at Goldstone, California, Using a 34-Meter Beam-Waveguide Antenna," TDA PR 42-132, October-December 1997, pp. 1-20, February 15, 1998.

National Aeronautics and Space Administration, "NASA Strategic Plan", NASA Policy Directive (NPD)-1000.1, Washington, DC, 1998.

Petty, S.M. and Clauss, R.C. "X-band Traveling Wave Maser," IEEE Transactions on Microwave Theory and Techniques," January 1968.

E. C. Posner and R. Stevens, "Deep Space Communication-Past, Present, and Future," IEEE Communications Magazine, May 1984.

W. Rafferty, et al, "Ground Antennas in NASA's Deep Space Telecommunications," Proceedings of the IEEE, May 1994.

E. Rechtin, "Communication Techniques for Space Exploration," IRE Transactions on Space Electronices and Telemetry," September 1959.

M. S. Reid, et al, "Low-Noise Microwave Receiving Systems in a Worldwide Network of Large Angennas," Proceedings of the IEEE, September 1973.

N. A. Renzetti, Ed, "A History of the Deep Space Network, From Inception to January 1, 1969, JPL TR 32-1533, September 1971.

Riley, A. L., S. Kayalar, A. Mittskus, D. Antsos, E. Grigorian, E. Olson, J. Neal, E. Satorius, and A. Kermode, "New Millennium Deep Space Tiny Transmitter: First Phase of a Digital Transponder," Proceedings of the AIAA/IEEE Digital Avionics Systems Conference, Atlanta, Georgia, pp 225-230, October 27-31, 1996.

T. Sato and C. T. Stelzried, "An Operational 960 Mc Maser System for Deep Space Tracking Missions," IRE Transactions on Space Electronics and Telemetry, June 1962.

Shannon, C. E., and W. Weaver, *The Mathematical Theory of Communications*, University of illionois Press, Urbana, Ill., 1959.

Shell, J., and R. B. Quinn, "A Dual-Cavity Ruby Maser for the Ka-Band Link Experiment," TDA PR 42-116, October-December 1993, pp. 53-70, February 15, 1994.

J. S. Shell, etal, "Ruby Masers for Maximum G/Top's," Proceedings of the IEEE, May 1994.

Stanton, P. and J. Chen, NPO-19907, NASA Tech Briefs, February, 1997.

C. T. Stelzried, et al, "Multi-feed Cone Cassegrain Antenna," U.S. Patent 3,534,375, Filed July 1968

R. Stevens and W. K. Victor, Eds, "The Goldstone Station Communications and tracking System for Project Echo, JPL TR 32-59, December 1960.

W.K. Victor and R. Stevens, "The 1961 JPL Venus Radar Experiment," IRE Transactions on Space Electronics and Telemetry, June 1962.

C. B. Waff, "The Road to the Deep Space Network." IEEE Speactrum, April 1993.

Wilson, K. E., and J. R. Lesh, "An Overview of the Galileo Optical Experiment (GOPEX)," The Telecommunications and Data Acquisition Progress Report 42-114, April-June 1993, pp. 192-204, August 15, 1993b.

Wilson, K. E., J. R. Lesh, K. Araki, Y. Arimoto, "Overview of the Ground-to-Orbit Lasercom Demo," Free-Space Laser Communication Technologies IX, Proceedings of SPIE, vol. 2990, pp 23-30, San Jose, California, 13-14 February, 1997b.

K. E. Wilson, J. R. Lesh, and T.-Y. Yan, The galileo optical experiment: a demonstration of deep space optical communications, in *Proc. Of SPIE OE/LASE 93,* Paper #1866-32, Los Angeles, CA, 1993a.

K. E. Wilson and J. R. Lesh, Overview of the Ground-to-Orbit Lasercom Demonstration, presented at the *CRL International Topical Workshop on Space Laser Communications,* Tokyo, Japan, 1997a.

Wozencraft, J. M. and I. M. Jacobs, *Principles of Communication Engineering* (Wiley, New York, 1965.

Yan, Tsun-Yee, Methu Jeganathan, and James Lesh, "Progress on the Development of the Optical Communications Demonstrator," Free-Space Laser Communication Technologies IX, Proceedings of SPIE, vol. 2990, p 94, San Jose, California, 13-14 February, 1997

J. H. Yuen. Ed. Deep Space Telecommunications Systems Engineering, Plenum, New York, 1983.

## NASA/JPL DSN and deep space missions key events

| Date | Event |
|---|---|
| Oct 1936 | First rocket propulsion experiment by Caltech T. von Karman in the Arroyo Seco north of the Rose Bowl near or on the present JPL location. |
| 1944 | JPL formed under CIT (California Institute of Technology) for U. S. Army contract activities |
| 1949 | Corporal mission selected for development as first U.S. guided missile weapons system. |
| May 1956 | Microlock ground station, first tests at Earthquake Valley near Julian, San Diego County, CA, 108 MHz |
| Jan 1958 | Explorer 1, first U.S. satellite, launched and tracked by JPL's Microlock ground system, 108 MHz, operated to May 1958. |
| Mar 1958 | Explorer 2 launched, earth satellite, failed |
| Mar 1958 | Explorer 3 launched, earth satellite, operated to June 1958. |
| July 1958 | Explorer 4 launched, earth satellite, operated to Oct 1958 |
| Aug 1958 | Explorer 5 launched, earth satellite, failed |
| Oct 1958 | Pioneer 1 launched, lunar mission, failed |
| Oct 1958 | NASA formed |
| Nov 1958 | Pioneer 2 launched, lunar mission, U.S. ARMY |
| Nov 1958 | Goldstone 'receiving' (Pioneer) station 26 m diameter polar mount antenna built |
| Dec 1958 | Pioneer 3 launched; failed to achieve escape velocity but discovered the second Van Allen radiation belt, L-band (960 MHz). |
| Mar 1959 | Elements of a Deep Space Tracking System described |
| Mar 1959 | Pioneer 4 launched, escaped to solar orbit, L-band |
| 1960-1965 | L-band cavity maser development with 17 to 30 K noise temperatures. |
| Feb 1960 | Goldstone 'transmitting' (Echo) station Az-El mount antenna built |
| Aug 1960 | Echo 1 launched with 960 MHz signal received at the Goldstone 'receiver' (Pioneer) station with S-band (2390 MHz) signal transmitted from the Goldstone 'transmitter' (Echo) station |
| Sept 1960 | First maser (R/D cavity type, open dewar, 960 MHz) installed on DSN Pioneer antenna |
| Feb 1961 | First S-band (2388 Mhz) maser (R/D cavity type, 25 K noise temperature with open dewar) installed on DSN Pioneer antenna |

| | |
|---|---|
| Mar 1961 | S-band Venus bistatic radar (transmit from the Echo site and receive from the Pioneer station) ; a successful planetary Venus return of the 2388 MHz signal represented the 1st ever successful planetary radar experiment. |
| Aug 1961 | Ranger 1 launch attempt, lunar prototype, launch failed. |
| Nov 1961 | Ranger 2 launch attempt, lunar prototype, launch failed. |
| Nov 1961 | 960 MHz maser system installed on the Pioneer station antenna for the Ranger 3 (RA-3) lunar probe 1/62 launch; during a critical maneuver near the Moon with the spacecraft antenna unfavorably oriented, this system received a satisfactory signal, unlike the Echo station system. |
| June 1962 | DSS 13 R/D single station planetary radar experiment successfully performed using uplink 100Kw in on-off mode with S-band. (2388 MHz) dual cavity maser with 18 K noise temperature cooled with closed cycle refrigerator. |
| 1962 | 26 m diameter polar mount antenna constructed at the Goldstone Echo (DSS 12) station. |
| 1962 | 26 m polar mount antennas completed for Woomera, Australia and Johannesburg, South Africa., completing the first 26m subnet. |
| Jan 1962 | Ranger 3 launched, lunar probe, spacecraft failed, missed moon. |
| April 1962 | Ranger 4 launched, lunar probe, spacecraft failed, impact moon. |
| June 1962 | 26 m az-el mount antenna moved from the Echo station to the Venus station. |
| July 1962 | Mariner 1 launched, Venus probe, failed. |
| Aug 1962 | Mariner 2 launched, Venus flyby 12/62, first spacecraft to fly to another Oct |
| 1962 | Ranger 5 launched, lunar probe, missed moon |
| 1963-1966 | S-band (2388 MHz) Traveling Wave Maser (TWM) development for radar applications with 8 K noise temperature. |
| 1963 | The NASA Advanced Systems Program was established, providing support for DSN research and development. |
| Jan 1963 | S-band 2 cavity maser reinstalled on the Venus station antenna for a Mars radar experiment. |
| Dec 1963 | DSN officially established. |
| 1963 | Completes pre-DSN history as defined for this study. |
| 1964-1971 | S-band (2295 MHz) TMW development for DSN missions support with 9 K noise temperature. |
| 1964 | DSN 64 m subnet initiated with the construction start of the Goldstone Mars station. |
| Jan 1964 | Ranger 6 launched, lunar probe, impact moon, cameras failed |
| July 1964 | Ranger 7 launched, lunar probe, successful, 4,308 pictures |
| Nov 1964 | Mariner 3 launched, Mars probe, shroud failed |
| Nov 1964 | Mariner 4 launched, Mars flyby July 1965 with 8.33 b/s data rate |
| 1965 | L-to S-band DSN frequency conversion completed to support the Mariners 3 and 4, the first S-band missions |
| 1965 | Second 26 m diameter polar mount antenna subnet completed with antennas at Goldstone, Tidbinbilla, Australia and Robledo, Spain. |
| Feb 1965 | Ranger 8 launched, lunar probe, successful, 7,317 pictures. |
| Mar 1965 | Ranger 9 launched, lunar probe, successful, 5,814 pictures. |
| 1966 | First signal received on the Goldstone 64 m antenna from Mariner 4 |
| May 1966 | Surveyor 1 launched, lunar lander, successful |
| Sept 1966 | Surveyor 2 launched, lunar lander, crashed |
| 1966-1968 | X-band (8450 MHz) TWM R/D development demonstration with 18K noise temperature performance for 26-and 64 m antenna applications. |
| 1966-1974 | S-band (2240-2420 MHz) TWM development for DSN missions support with 4-6 K noise temperatures |
| April 1967 | Surveyor 3 launched, lunar lander, successful |
| June 1967 | Mariner 5 launched. Venus flyby Oct 1967 |

| | |
|---|---|
| June 1967 | X-band feedcone constructed to test DSS 13 and DSS 14 suitability at 8.4 GHz. |
| July 1967 | Surveyor 4 launched, lunar lander, crashed |
| Sept 1967 | Surveyor 5 launched, lunar lander, successful |
| Nov 1967 | Surveyor 6 launched, lunar lander, successful |
| 1968 | Goldstone 64 m diameter antenna modified from single to multiple feedcone configuration; later implemented throughout the 64 m subnet. |
| Jan 1968 | Surveyor 7 launched, lunar lander, successful |
| Nov 1968 | First ever successful CW signal Faraday Rotation radio science experiment in the Solar corona using the Goldstone 64 m diameter DSS 14 antenna tracking polarization of the Pioneer 6 linearly polarized signal during a Solar occultation |
| Feb 1969 | Mariner 6 launched, Mars flyby 7/69 |
| Mar 1969 | Mariner 7 launched, Mars flyby 8/69 |
| 1970 | S-band (2285 MHz) TWM development for DSN missions support with 5 K noise temperatures |
| 1970-1972 | DSS 14 tunable X-band (7600-8900 Mhz) TWM development for VLBI application with 7-13 K noise temperatures |
| May 1971 | Mariner 8 launch attempt to Mars, failed |
| May 1971 | Mariner 9 launched, Mars orbiter 11/13/71 to 10/27/72 |
| 1971-1980 | DSS 14 tunable R/D Ku-band (14.3-16.3 GHz) TWM development for antenna evaluation and radio astronomy with 7-13 K noise temperatures |
| Mar 1972 | Pioneer 10 launched |
| 1973-1989 | X-band (8400-8440 MHz) TWM development DSN missions support with 8 K noise temperatures |
| 1973 | Both the Australian and Spain 64 m diameter antennas built to complete the world wide 64 m subnet. |
| 1973 | Goldstone 64 m diameter antenna tricone upgraded with dichroic plate feed optics to permit simultaneous S-and X-band reception as well as S-band uplink; later capability extended to the 64 m subnet. |
| Nov 1973 | Mariner 10 (Mariner Venus Mercury-73) launched to Venus and Mercury as first dual-planet mission. S-band and first deep space use of experimental X-band downlink |
| 1974 | Tunable S-band (2250-2400 MHz) TWM development for DSN missions support with 2-4 K noise temperatures |
| Aug 1975 | Viking 1 launched, Mars orbiter/lander, orbit 6/76, landing 7/76, S-band and experimental X-band |
| Sept 1975 | Viking 2 launched, Mars orbiter/lander, orbit 8/76, landing 9/76, S-band and experimental X-band |
| Aug 1977 | Voyager 2 launched, Jupiter 7/79, Saturn 8/81, Uranus 1/86, Neptune 8/89, continues on interstellar mission, S-and X-bands |
| Sept 1977 | Voyager 1 launched, Jupiter 3/79, Saturn 11/80, continues on interstellar mission, S-and X-bands |
| May 1978 | Pioneer Venus 1 launched. |
| Aug 1978 | Pioneer Venus 2 launched |
| Mar 1979 | Voyager 1 Jupiter encounter |
| July 1979 | Voyager 2 Jupiter encounter |
| 1979 | The DSN 26 m polar-mount antennas expanded to 34 m diameter and X-band receive added in preparation for the Voyager 1 Saturn encounter; these antennas referred to as 'standards' (STD's). |
| 1980- | X-band (8400-8500MHz) TWM for Voyager support with 3-4.5 K noise temperatures |

| | |
|---|---|
| Nov 1980 | Voyager 1 Saturn Encounter at 10 AU with array of the 64 m with improved efficiency and 34 m STD's with lower noise Block 2 masers for overall 2 dB link improvement resulting in 44 kb/s downlink data rate. |
| Nov 1980 | Voyager 1 swings out of the ecliptic plane and starts journey beyond the solar system |
| 1981- | Tunable K-band (18-25 GHz) R/D Reflected Wave Maser (RWM) for Radio Astronomy support with the 64 m antenna subnet with 12 K LNA noise temperatures. |
| 1981 | Pioneer station decommissioned |
| 1985- | S-band (2210-2320 MHz) TWM for DSN support of the International Cometary Explorer (IC) mission with 3-5 K LNA noise temperatures |
| 1985 | A DSN subnet of 34 m diameter High Efficiency (HEF) dual shaped reflector antennas with S/X single feedhorn (common aperture) completed in preparation for the Voyager 2 Uranus encounter |
| 1985 | Goldstone Pioneer station designated a national monument |
| Jan 1986 | Voyager 2 Uranus encounter at 19 AU, arrayed using 64 m's, STD's and 34 m HEF's for 29.9 kb/s data rate. |
| 1988 | The DSN 64 m subnet upgrade to high efficiency dual shaped reflector 70 m diameter antennas providing 2 dB improved X-band link capability for the Voyager Neptune encounter completed. |
| May 1989 | Magellan launched to Venus, orbited 8/90 to 10/94, mapping 99% of planet. |
| Aug 1989 | Voyager 2 Neptune Encounter, arraying multiple DSN and non-DSN antennas for nearly 8 dB improvement relative to a single earlier DSN 64 m antenna configuration. |
| Oct 1989 | Galileo launched, Jupiter orbiter/probe, arrived 12/95, S-and X-bands |
| Jan 1990-2020 | Voyager Interstellar Mission (VIM), Voyager 1 and 2 extended mission |
| Oct 1990 | Ulysses launched, repeated solar poles flyby's mission, S-and X-bands. |
| 1991 | Venus station BWG antenna installation of X-band (8500 MHz) TWM with open cycle super cooled to 1.7 K providing 2.5 K LNA noise temperature performance for use with the Goldstone radar system (transmitting from the 70 m DSS 14 antenna). |
| Sept 1992 | Mars Observer launched (mission failed 8/93 before entering Mars orbit insertion) |
| 1992-1993 | Tunable 'open cycle' DSS 13 R/D Ka-band (33.3-34.0) dual cavity maser for Mars Observer Ka Band Link Experiment (KABLE-1) support providing 5 K LNA noise temperatures performance. |
| 1994 | DSS 24, the first DSN 34 m diameter dual shaped reflector beamwaveguide (BWG) with large electronics 'pedestal room' was completed at Goldstone. |
| Oct 1994 | Magellan ended Venus mapping mission by dipping into the atmosphere as aerobraking test; since used by other planetary missions |
| Nov 1995 | Radarsat launched, S-band, included JPL Summer Undergraduate Research Fellowship Satellite-1 (Surfsat-1) experimental satellite with X-and Ka-bands. |
| Feb 1996 | Near-Earth Asteroid Rendezvous (NEAR) launched, X-band |
| Nov 1996 | Mars Global Surveyor (MGS) launched, Mars orbit on 9/97, X-band. |
| Dec 1996 | Mars Pathfinder launched and put a lander and rover on Mars July 4, 1997 with data ending 9/97. |
| Oct 1997 | Cassini launched, en route to Saturn, arrive 2004. |
| Jan 1998 | Lunar Prospector launched, S-band |
| Feb 1998 | Voyager 1 passed Pioneer 10 to become the most distant human-made object in space |
| Oct 1998 | Deep Space 1 launched, testing ion engine and other technologies, including experimental Ka-band (32.16 GHz), X-band prime. |

| | |
|---|---|
| Dec 1998 | Mars Climate Orbiter launched, enroute to Mars, arrival 9/99, X-band |
| Jan 1999 | Mars Polar Lander launched, enroute to Mars, arrival 12/99, X-band |
| Mar 1999- | Tunable 'open cycle' DSS 13 R/D Ka-band (33.3-34.0) dual cavity maser with added dual polarization capability for radio astronomy spectral line search providing 5 K LNA noise temperature. |
| Mar 1999 | Wide Field Infrared Explorer (WIRE) launched to Sun-synchronous near-polar orbit, failed, S-band |
| **Future:** | |
| Oct 1999 | Galileo flyby of Io. |
| 2001 | Radioastron (SVLBI) launch, X (8.5 GHz)-and Ku (14 and 15 GHz)-bands tracking with L (1.6 GHz)-and K-(22 GHz) band co-observing DSN support. |
| Mar 2001 | Pluto Express launch with two spacecraft to flyby Pluto in 2013 with several months playback to the DSN. |
| Nov 2903 | Solar Probe launch with close approach to the Sun in 2007. |
| June 2004 | Cassini Saturn arrival |